Squaramide-based supramolecular materials for 3D cell culture applications

Tong, C.

Citation

Tong, C. (2021, March 10). *Squaramide-based supramolecular materials for 3D cell culture applications*. Retrieved from https://hdl.handle.net/1887/3151624

Version:	Publisher's Version
License:	[Licence agreement concerning inclusion of doctoral thesis in the Institutional Repository of the University of Leiden](#)
Downloaded from:	[https://hdl.handle.net/1887/3151624](#)

Note: To cite this publication please use the final published version (if applicable).

Cover Page

The handle https://hdl.handle.net/1887/3151624 holds various files of this Leiden University dissertation.
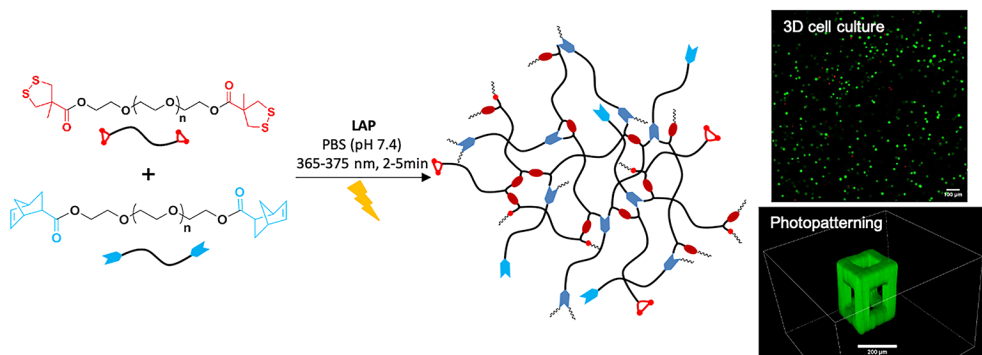
Author: Tong, C.
Title: Squaramide-based supramolecular materials for 3D cell culture applications
Issue Date: 2021-03-10

CHAPTER 4

Photopatternable, branched polymer hydrogels based on linear macromonomers for 3D cell culture applications

This chapter was prepared as an original research paper: Ciqing Tong, Joeri A. J. Wondergem, Doris Heinrich and Roxanne E. Kieltyka, *ACS Macro Lett.* **2020**, *9*, 882-888.

4.1 Abstract

Photochemical ligation strategies in hydrogel materials are crucial to model spatiotemporal phenomena that occur in the natural extracellular matrix. We here describe the use of cyclic 1,2-dithiolanes to cross-link with norbornene on linear poly(ethylene glycol) polymers through UV irradiation in a rapid and byproduct-free manner, resulting in branched macromolecular architectures and hydrogel materials from low-viscosity precursor solutions. Oscillatory rheology and NMR data indicate the one-pot formation of thioether and disulfide cross-links. Spatial and temporal control of the hydrogel mechanical properties and functionality was demonstrated by oscillatory rheology and confocal microscopy. A cytocompatible response of NIH 3T3 fibroblasts was observed within these materials, providing a foothold for further exploration of this photoactive cross-linking moiety in the biomedical field.

4.2 Introduction

Synthetic hydrogels have gained attention as scaffolds to mimic the 3D microenvironment of cells in vitro thanks to their water-rich character in conjunction with their tunable chemical and physical properties.[1] To this end, highly hydrophilic poly(ethylene glycol) (PEG)-based polymers combined with various cross-linking methods (e.g., photo-polymerization, chemoselective ligation, enzyme-mediated cross-linking) have been exploited to prepare hydrogels for 3D cell culture for a diverse array of cell types and aims.[2-4] Most reported examples are based on branched (multiarmed or star) precursors; far fewer involve cross-linking of end functionalized linear chains that are synthetically accessible, but typically require additional components to form gel-phase materials.[5-11] Therefore, bio-orthogonal and atom-efficient cross-linking chemistries that provide handles for external control of the reaction rate remain attractive to form and modulate hydrogel properties in the biomedical area.[12-14]

Thiol-based chemistries have seen extensive use in the polymer field for the vulcanization of rubbers and more recently, for bioconjugation.[15-18] As an alternative to metal based bioconjugations, thiol-X reactions have grown in use because of their efficiency under mild reaction conditions, following either a nucleophilic addition-elimination or a radical mechanism. Both mechanisms have been applied in the hydrogel field,[19,20] the latter often being initiated by photo-activation to enable chemical cross-linking or polymerization.[21-23]

A drawback to the use of thiols is that their reactivity often results in disulfide formation during storage, which can be problematic for their subsequent application.[24] Consequently, protected and latent thiols are being increasingly used in polymer materials to gain control over their properties.[24] Thiol protection strategies based on linear disulfides are atom-inefficient, releasing small molecules that can leach out of the material or require additional purification steps, which could be problematic for use in the biomedical field.[24] In contrast, latent thiols that reveal the reactive moiety on demand are highly attractive because of their atom-efficient nature and lack of byproducts. In the polymer chemistry field, cycles based on carbon-sulfur bonds (e.g., thiolactones, Traut's reagent) have been extensively explored as latent thiols,[24] whereas far fewer examples involving cyclic disulfides (e.g., 1,2-dithiolanes, 1,2-dithianes)[25-30] have been reported. The latter can be especially beneficial in gel phase materials, thanks to their capacity to act as bifurcated cross-linkers or cargo attachment points providing two reactive thiol moieties on ring opening.[31-34] Thus far, most

approaches using cyclic disulfides use conditions that favor nucleophilic addition-elimination, resulting in materials that require additional small molecule reagents for their stabilization and can prove challenging for their application in biomaterials.[31,32]

In this study, we exploit the instability of 1,2-dithiolanes (DT) using methyl asparagusic acid (**Figures S4.1** and **S4.2**) with UV light at 365-375 nm to prepare hydrogel materials with spatiotemporal control over their properties in an atom-efficient manner. We specifically examine their introduction on linear PEG polymers to understand their capacity to prepare light-responsive hydrogel materials for 3D cell culture (**Figure 4.1**) in an easy and economic way.
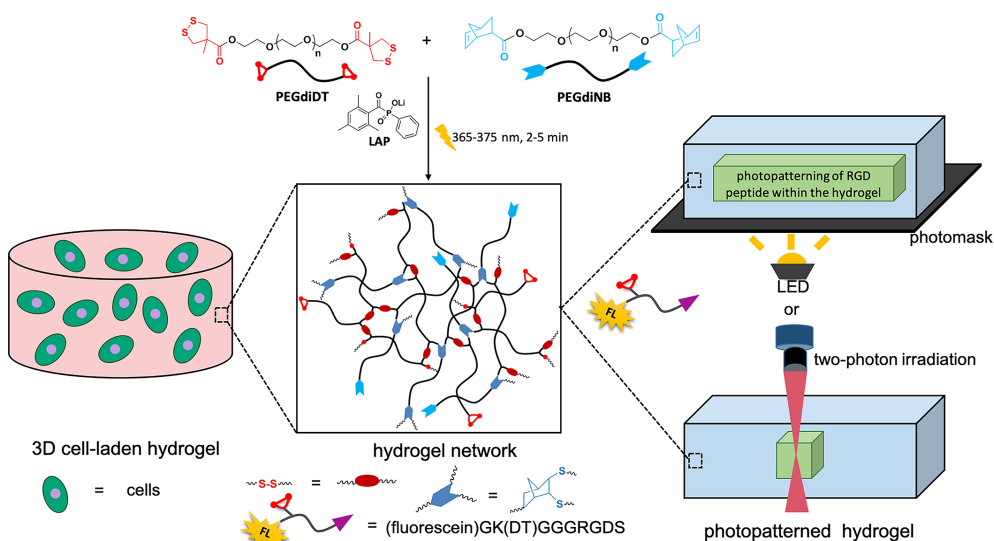

Figure 4.1 Photoreaction of DT and NB polymers in the presence of a cell suspension results in hydrogels with cells encapsulated in 3D. They can be further patterned with a fluorescently-labelled RGD peptide using a photomask during UV irradiation or two-photon laser lithography.

4.3 Results and discussion

4.3.1 Synthesis of PEG polymers and preparation of hydrogels

Linear PEG polymers (**PEGdiDT**, **PEGdiNB**) were synthesized by a one-step reaction using carbodiimide coupling chemistry resulting in a high degree of end-functionalization (ca. 100%; **Figures S4.3** and **S4.5**). To examine the potential for UV-mediated cross-linking of the DT moiety, UV irradiation at either 365 or 375 nm (depending on the light source) was applied, using the absorption of DT that has a maximum at 330 nm. Importantly, irradiation of the linear macromonomer

PEGdiDT on its own or in combination with linear **PEGdiNB** and a photoinitiator, lithium phenyl-2,4,6-trimethylbenzoyl-phosphinate (**LAP**), resulted in hydrogel materials starting from low viscosity precursor solutions (*vide infra*).

4.3.2 Characterization of hydrogels

Oscillatory rheology was used to evaluate the gelation rate and mechanical properties of the photo-cross-linked DT-NB PEG hydrogels. Because of the known capacity of the DT moiety to form disulfide cross-links or undergo polymerization on its own in the presence of nucleophiles, heat or light,[33,35,36] we first evaluated the capacity of the **PEGdiDT** polymer to cross-link with itself prior to the addition of **PEGdiNB**. **PEGdiDT** (6.0 mM) required more than 15 min UV irradiation to yield a viscous solution, and 30 min for a weak hydrogel (storage modulus G′ = 42 ± 6 Pa). Moreover, the addition of **LAP** (1.0 mM) to **PEGdiDT** did not yield a hydrogel despite its reaction with DT (*vide infra*). Thus, the inefficient gelation of **PEGdiDT** on its own could be challenging for applications involving 3D cell culture.

In contrast, replacing half of the macromonomer (3.0 mM) with **PEGdiNB** and using **LAP** (1.0 mM) resulted in a drastic reduction of the gelation time (less than 2 min) and a substantial increase of the storage modulus (G′ = 1265 ± 62 Pa; **Figure 4.2A**). Without **LAP,** no hydrogel was formed after 30 min UV irradiation (**Figure 4.2A**). Also, no hydrogel was formed when cross-linking was attempted with **PEGdiSH** and **PEGdiNB** as a control, unless a multi-arm cross-linker (**PEG4SH**) was used, pointing out the importance of DT for network formation from linear macromonomers (**Figure S4.8**). Moreover, increasing the total polymer concentration (from 4.0 to 16.0 mM) while maintaining an equimolar DT/NB ratio and constant **LAP** concentration (1.0 mM) resulted in highly efficient hydrogel formation, with G′ at the plateau rising from 167 ± 11 Pa to 20018 ± 1781 Pa (**Figures 4.2B** and **S4.9**). Hence, DT can efficiently form hydrogels with NB on linear macromonomers upon light irradiation in the presence of a photoinitiator at a rate that is attractive for use in 3D cell culture.
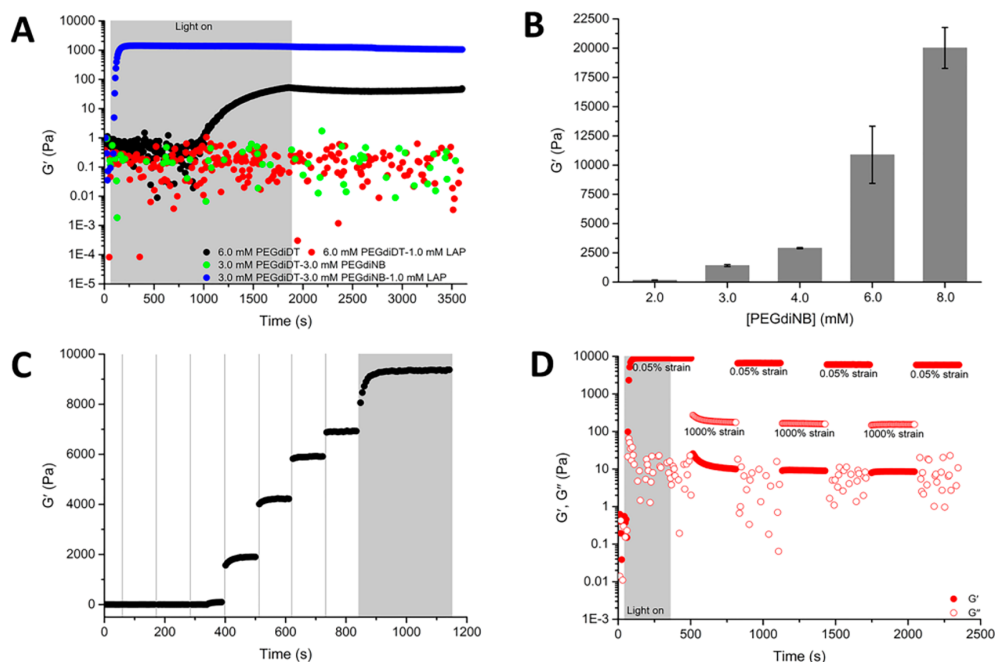
Figure 4.2 (A) Averaged (N = 3) time sweep of **PEGdiDT** hydrogels and **PEGdiDT**-**PEGdiNB** hydrogels without and with **LAP** (1.0 mM) using 30 min UV irradiation during the measurement (γ = 0.05%, f = 1.0 Hz) at room temperature. (B) The plateau storage moduli (G') of hydrogels **PEGdiDT**-**PEGdiNB** with **LAP** (1.0 mM) were tuned by adjusting the total polymer concentration and keeping the ratio of [NB]/[DT] (1:1) constant (under 5 min UV irradiation). (C) Step UV-light irradiation of a hydrogel containing 6.0 mM **PEGdiDT**-6.0 mM **PEGdiNB**-1.0 mM **LAP**. (D) Averaged (N = 3) step-strain measurement of hydrogel (6.0 mM **PEGdiDT**-6.0 mM **PEGdiNB**-1.0 mM **LAP**) after 5 min UV irradiation. For all data, UV-light irradiation condition: 10 mW/cm^2, wavelength: 320-500 nm, primary peak: 365 nm. The shaded part of the data indicates when light was applied. Error bars were calculated according the average of repeat measurements (N $\geq$ 3).

To better understand the scope of the photoactivated one-pot DT-NB reaction for the preparation of hydrogels, we measured their rheological properties while tuning the **LAP** concentration, light intensity, step light irradiation time, and [NB]/[DT] ratio (**Table S4.1**). Using the lowest **LAP** concentration (0.1 mM) and 5 min UV irradiation, no gelation was observed. Increasing **LAP** (1.0 mM), provided a higher rate of gel formation and an increase in G', while higher **LAP** concentrations (4.0 mM) did not yield a greater increase in G' (**Figure S4.10**). A higher intensity of the light source (~30.0 mW/cm^2) increased the rate of gel formation in comparison to lower values (~5.0 mW/cm^2, ~10.0 mW/cm^2), but in all cases, a comparable G' was eventually reached (**Figure S4.11**). Moreover, the G' of the hydrogels can be modulated in a stepwise fashion using UV irradiation in intervals, demonstrating the potential of this chemistry for

applications where spatial or temporal control is desired (**Figure 4.2C**). Increasing the concentration of DT relative to NB ([NB]/[DT] from 2:1 to 1:2) resulted in hydrogel formation and an increase in G', while further increasing DT ([NB]/[DT] = 1:3) resulted in a slower gelation rate and decreased G' (**Figure S4.12**).

To probe the contribution of the reversible covalent cross-links between the DT moieties to the properties of the DT-NB hydrogels, we evaluated their potential for self-recovery through a step-strain experiment. All hydrogels showed a recovery of 50-70% of the original G' after the application of high strain, with the recovery increasing with DT concentration due to an increase in the number of dynamic disulfide cross-links in the network (**Figures 4.2D** and **S4.13**).

Scanning electron microscopy was performed to gain insight into the hydrogel microstructure. A macroporous structure of the **PEGdiDT**-**PEGdiNB** hydrogel was observed, consistent with other covalent polymer hydrogels (**Figure S4.14**). Additionally, to shed light on the degradation kinetics of the **PEGdiDT** and **PEGdiDT**-**PEGdiNB** hydrogels, their swelling ratio was examined at various [NB]/[DT] ratios at different time points (**Figure S4.15**). The swelling ratio of the DT-NB hydrogel for [NB]/[DT] ratios of comparable G' remained largely unchanged after 9 days in PBS or cell culture media (DMEM) at 37 °C. Conversely, **PEGdiDT** hydrogels degraded within 24 h, highlighting the importance of using NB in the polymer networks to enable their use for cell culture applications.

Collectively, these results suggest that the irradiation of DT with UV light forms both thioether and disulfide bonds due to the reaction of the NB and DT units, respectively, enabling the formation of hydrogel materials from linear polymer precursors that are inaccessible using linear disulfides or monothiols.

4.3.3 Understanding the DT-NB reaction using ^{1}H-NMR

To further understand the DT-NB reaction on the PEG macromonomers in the presence of **LAP**, ^{1}H-NMR spectroscopy was performed in D_2O. Monofunctional linear polymers (**PEGmDT** and **PEGmNB**, **Figures S4.4** and **S4.6**) were synthesized starting from O-methyl-undecaethylene glycol in an effort to avoid hydrogel formation during the reaction and to simplify NMR analysis. UV light activation of **PEGmDT** or **PEGmNB** on their own, with and without **LAP** was first examined (**Figures S4.16-S4.24** and **Tables S4.2** and **S4.3**). For all reactions, the -CH$_3$ peak (~3.35 ppm) of O-methyl-undecaethylene glycol was selected as a reference, and changes in the -CH$_2$ (~3.01-3.04 ppm) and -CH$_3$ (~1.49 ppm) peaks of the DT and the -ene proton signals (~5.92-6.24 ppm, range a) of NB were used to calculate

the conversion of DT and NB, respectively, during the reaction. Whereas no change in the ^{1}H-NMR spectrum for **PEGmNB** was observed, even after 30 min UV light, irradiation of **PEGmDT** for 5-30 min resulted in the formation of multiple new peaks (~1.99-3.30 ppm, range b; and ~1.00-1.98 ppm, range c) upfield of the -CH$_2$ and -CH$_3$ resonances of DT, suggestive of its ring-opening polymerization. Addition of an increasing concentration of **LAP** to either **PEGmNB** or **PEGmDT** accelerated the consumption of NB (e.g., ~3% conv. for 1.0 mM **LAP** and ~47% conv. for 10.0 mM **LAP**) and DT (~17% conv. for 1.0 mM **LAP** and ~72% conv. for 10.0 mM **LAP**) with short UV irradiation times (5 min), pointing out the reaction of the initiator with both of the individual components. This result is consistent with an earlier report by Anseth's lab. that showed that high concentrations of **LAP** can consume the disulfides of hydrogel precursors.[37]

Using an equimolar solution of **PEGmNB** and **PEGmDT** with 5 min UV irradiation resulted in increased conversion with higher **LAP** concentrations (0.1 mM **LAP**: ~3-16% conv. of NB and ~12-19% conv. of DT; 1.0 mM **LAP**: ~80-86% conv. of NB and ~100% conv. of DT). New peaks were found to appear between 2.0 and 3.0 ppm, as previously reported for thioether α-protons,[23] further confirming the bond formation between the DT and NB units. Substantial broadening of all peaks in the NMR spectrum suggested the polymerization of both components (**Figures 4.3** and **S4.25** and **Table S4.4**).

In a second step, we evaluated the photoinitiated DT-NB reaction with **LAP** (1.0 mM) at different [NB]/[DT] ratios (2:1 to 1:2) to gain insight into cross-links that drive the formation of the hydrogel material (**Figures S4.26** and **S4.27** and **Table S4.4**). Complete NB conversion (from 43% to 100%) after 5 min UV irradiation was obtained when increasing the DT concentration. This result shows that an excess of DT is necessary to fully cross-link NB and suggests that disulfide bond formation, and inactivation of DT by **LAP** occur in parallel in the hydrogel.

As a control experiment, we compared the integration of regions a-c from the DT-NB reaction against a reaction of **PEGmNB** with DL-dithiothreitol (**DTT**), a dithiol reagent that forms hydrogen radicals with UV light (5.0 mM **DTT**-10.0 mM **PEGmNB**-1.0 mM **LAP**, **Figure S4.28**). After 5 min irradiation, a decrease in the integrated area of range a, followed by a symmetrical increase in the integrated areas of ranges b and c were observed (**Table S4.5**). This result is consistent with a thiol-ene reaction, where the loss of the NB-ene signals in range a (signals 1 and 2) and the simultaneous formation of a single thioether linkage in range b (signal 1') and a -CH$_2$- group in range c (signal 2') are expected upon UV light irradiation.[23] In

comparison, in the DT-NB reaction, the reduction of the integrated area of range a (disappearance of the -ene in NB) and the concomitant increase of range b while range c remains unchanged, suggest the formation of two thioether bonds on NB (**Table S4.4**). This result is made possible by the lack of abstractable -SH protons and the formation of two thiyl radicals with UV light on the DT moiety.
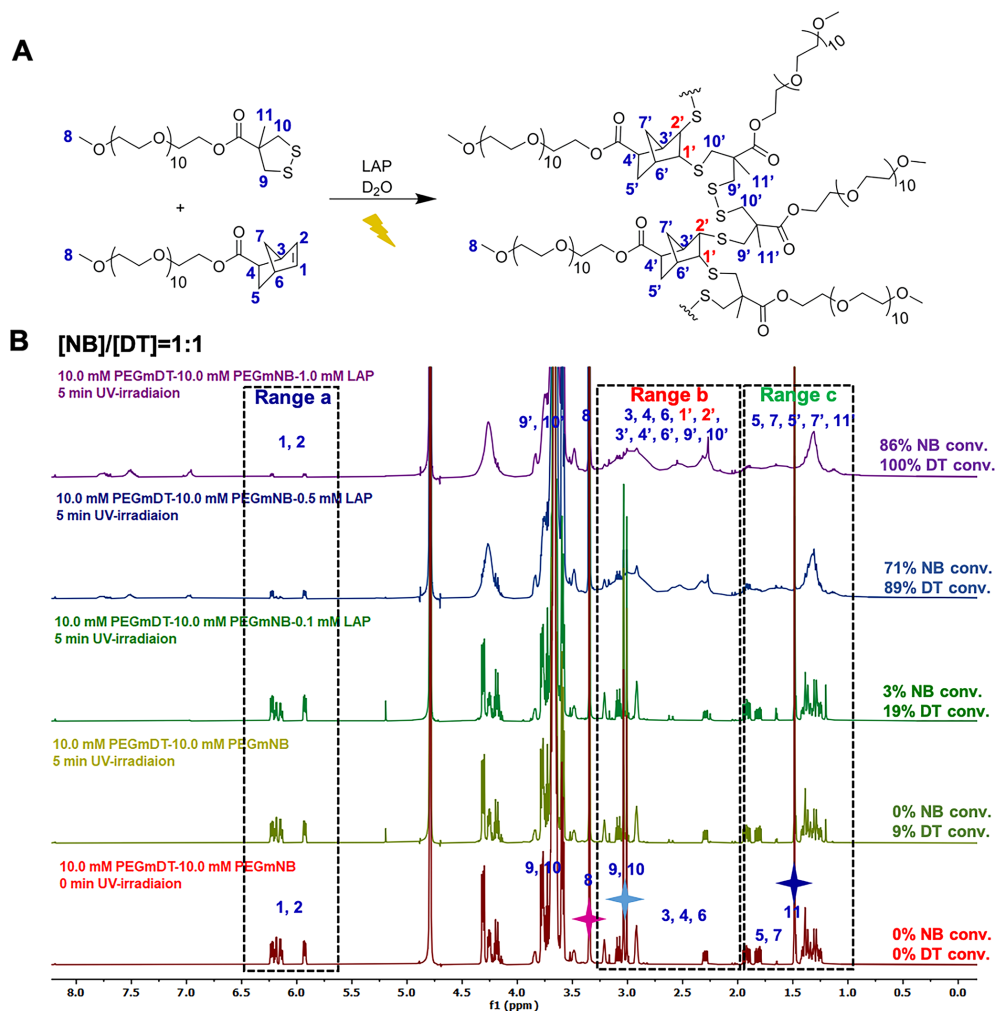

Figure 4.3 (A) Proposed reaction product of **PEGmDT** and **PEGmNB**, including double substitution of norbornene and disulfide cross-links, based on ^{1}H-NMR and oscillatory rheology. (B) ^{1}H-NMR (400 MHz) spectra in D_2O of the **PEGmDT-PEGmNB** reaction ([NB]/[DT] = 1:1) with different concentrations of **LAP** (0, 0.1, 0.5, and 1.0 mM) without and with 5 min UV irradiation using a benchtop LED (~10 mW/cm^2, 375 nm).

4.3.4 3D cell culture study

We then examined the potential for application of the DT-NB reaction for 3D cell culture applications by encapsulating NIH 3T3 fibroblasts in the hydrogel materials. Initial gel inversion experiments showed that **PEGdiDT**-**PEGdiNB** hydrogels were formed in cell culture media (**Figure S4.7**), opening the door for further experiments involving cells. When hydrogels consisting of 2.0 mM **PEGdiDT**-2.0 mM **PEGdiNB**/1.0 mM **LAP** were irradiated with UV light for 2 minutes, largely viable cell populations (>91%) were observed in a LIVE/DEAD assay after 24 and 48 h (**Figure S4.29**). However, increasing the overall polymer concentration (6.0 mM) decreased cell viability to ~80% after 48 h culture (**Figures 4.4A** and **4.4 B**). Generally, a cytocompatible response of NIH 3T3 cells in the presence of the DT-NB cross-linking reaction was found.

4.3.5 Photopatterned cell-adhesive peptide in hydrogel

Next, we further examined the potential of the DT-NB reaction for spatial and temporal photopatterning of hydrogel materials for cell culture applications. A fluorescein dye- and DT-labeled cell-adhesive RGD peptide, **(fluorescein)GK-(DT)GGGRGDS** (**Figure 4.4C**), was synthesized to visualize and study the possibility of UV-light-activated coupling between the hydrogel and functional peptides, such as RGD. After initial UV exposure to form the hydrogel, secondary illumination through a photomask produced RGD-hydrogel patterns with cell-size features throughout the volume of the gel (**Figure S4.30**). Moreover, the low near-infrared absorbance of the hydrogel enables full spatial control over peptide-gel photo coupling by two-photon laser lithography (**Figure 4.4D**). Using this technique, 3D peptide patterns can be laser-written into the gel at cell-sized relevant length scales (1-100 μm), highlighting the potential to introduce the RGD peptide or other bioactive cues spatially and temporally in a user-defined manner.
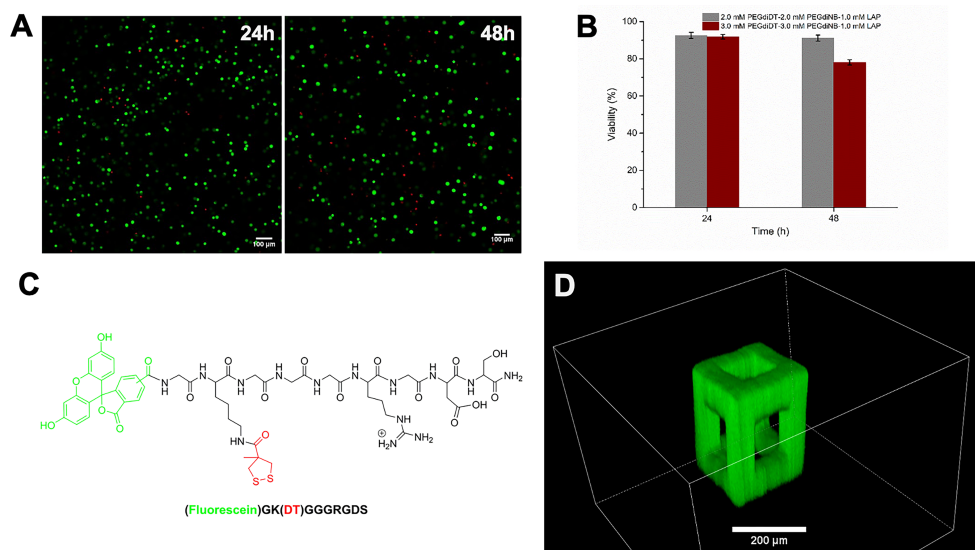
Figure 4.4 (A) Representative confocal microscopy images of NIH 3T3 cells after 24 and 48 h encapsulated in 3D of the DT-NB hydrogel (3.0 mM **PEGdiDT**-3.0 mM **PEGdiNB**-1.0 mM **LAP**) with 2 min UV irradiation using a benchtop LED (∼10 mW/cm^2, 375 nm). Scale bar: *100 µm*. Green: *viable cells*, red: *dead cells*. (B) Averaged (N = 3) cell viabilities of NIH 3T3 cells at 24 and 48 h. Error bars represent the standard deviation of independent samples. (C) Chemical structure of the fluorescein-labeled cell-adhesive RGD peptide: **(fluorescein)GK(DT)GGGRGDS**. (D) Confocal microscopy image of two-photon cross-linked and a bound cell-adhesive peptide through DT-NB (3.0 mM **PEGdiDT**-3.0 mM **PEGdiNB**-1.0 mM **LAP**) via direct-laser writing. Scale bar: *200 µm*.

4.4 Conclusions

In summary, we here demonstrate the use of a cyclic disulfide, DT, as a latent thiol that participates in highly efficient and byproduct-free light-mediated reaction with NB in the presence of a photoinitiator to form cytocompatible hydrogel materials. The DT moiety yields a bifurcated crosslinker through ring opening upon light activation, that can efficiently crosslink with itself and with NB forming both reversible and irreversible crosslinks and materials with self-healing character in one-pot. Importantly, linear polymer precursors can be used to prepare hydrogels using the reaction between DT and NB, and their mechanics or functionality can be controlled spatiotemporally using light. Hence, we envisage that the combination of these units can open the door to exploit the use of linear polymer scaffolds that are synthetically accessible and economical for manifold biomedical applications involving cells.

4.5 References

(1) Huang, G.; Li, F.; Zhao, X.; Ma, Y.; Li, Y.; Lin, M.; Jin, G.; Lu, T. J.; Genin, G. M.; Xu, F. *Chem. Rev.* **2017**, *117* (20), 12764-12850.

(2) Zhu, J. *Biomaterials* **2010**, *31* (17), 4639-4656.

(3) Lin, C. C. *RSC Adv.* **2015**, *5* (50), 39844-398583.

(4) Liu, S. Q.; Tay, R.; Khan, M.; Rachel Ee, P. L.; Hedrick, J. L.; Yang, Y. Y. *Soft Matter* **2010**, *6* (1), 67-81.

(5) He, L.; Szopinski, D.; Wu, Y.; Luinstra, G. A.; Theato, P. *ACS Macro Lett.* **2015**, *4* (7), 673-678.

(6) Casuso, P.; Perez-San Vicente, A.; Iribar, H.; Gutierrez-Rivera, A.; Izeta, A.; Loinaz, I.; Cabanero, G.; Grande, H. J.; Odriozola, I.; Dupin, D. *Chem. Commun.* **2014**, *50* (96), 15199-15201.

(7) Wang, D.; Yang, X.; Liu, Q.; Yu, L.; Ding, J. *J. Mater. Chem. B* **2018**, *6* (38), 6067-6079.

(8) Ren, K.; Li, B.; Xu, Q.; Xiao, C.; He, C.; Li, G.; Chen, X. *Polym. Chem.* **2017**, *8* (45), 7017-7024.

(9) Moriyama, K.; Wakabayashi, R.; Goto, M.; Kamiya, N. *Biochem. Eng. J.* **2015**, *93*, 25-30.

(10) Nguyen, Q. T.; Hwang, Y.; Chen, A. C.; Varghese, S.; Sah, R. L. *Biomaterials* **2012**, *33* (28), 6682-6690.

(11) Cruise G.M.; Scharp D. S.; Hubbell J. A. *Biomaterials* **1998**, *19*, 1287-1294.

(12) Kharkar, P. M.; Kiick, K. L.; Kloxin, A. M. *Chem. Soc. Rev.* **2013**, *42* (17), 7335-7372.

(13) Seliktar D. *Science* **2012**, *336*, 1124-1128.

(14) Azagarsamy, M. A.; Anseth, K. S. *ACS Macro Lett.* **2013**, *2* (1), 5-9.

(15) Stenzel, M. H. *ACS Macro Lett.* **2012**, *2* (1), 14-18.

(16) Hoyle, C. E.; Lowe, A. B.; Bowman, C. N. *Chem. Soc. Rev.* **2010**, *39* (4), 1355-1387.

(17) Boyd, D. A. *Angew. Chem. Int. Ed.* **2016**, *55* (50), 15486-15502.

(18) Hoyle, C. E.; Bowman, C. N. *Angew. Chem. Int. Ed.* **2010**, *49* (9), 1540-1573.

(19) Mutlu, H.; Ceper, E. B.; Li, X.; Yang, J.; Dong, W.; Ozmen, M. M.; Theato, P. *Macromol. Rapid Commun.* **2019**, *40* (1), e1800650.

(20) Su, J. *Gels* **2018**, *4* (3), 72.

(21) Perera, M. M.; Ayres, N. *Polym. Chem.* **2017**, *8* (44), 6741-6749.

(22) Nimmo, C. M.; Shoichet, M. S. *Bioconjug Chem.* **2011**, *22* (11), 2199-2209.

(23) Fairbanks, B. D.; Schwartz, M. P.; Halevi, A. E.; Nuttelman, C. R.; Bowman, C. N.; Anseth, K. S. *Adv. Mater.* **2009**, *21* (48), 5005-5010.

(24) Goethals, F.; Frank, D.; Du Prez, F. *Prog. Polym. Sci.* **2017**, *64*, 76-113.

(25) Fang, J.; Ye, S. H.; Wang, J.; Zhao, T.; Mo, X.; Wagner, W. R. *Biomacromolecules* **2015**, *16* (5), 1622-1633.

(26) Tang, H.; Tsarevsky, N. V. *Polym. Chem.* **2015,** *6* (39), 6936-6945.

(27) Sakai, N.; Matile, S. *J. Am. Chem. Soc.* **2011**, *133* (46), 18542-18545.

(28) Morelli, P.; Matile, S. *Helv. Chim. Acta* **2017**, *100* (3), e1600370.

(29) Hu, J.; Wu, T.; Zhang, G.; Liu, S. *J. Am. Chem. Soc.* **2012**, *134* (18), 7624-7627.

(30) Margulis, K.; Zhang, X.; Joubert, L. M.; Bruening, K.; Tassone, C. J.; Zare, R. N.; Waymouth, R. M. *Angew. Chem. Int. Ed.* **2017**, *56* (51), 16357-16362.

(31) Yu, H.; Wang, Y.; Yang, H.; Peng, K.; Zhang, X. *J. Mater. Chem. B* **2017**, *5* (22), 4121-4127.

(32) Barcan, G. A.; Zhang, X.; Waymouth, R. M. *J. Am. Chem. Soc.* **2015**, *137* (17), 5650-5653.

(33) Song, L.; Zhang, B.; Gao, G.; Xiao, C.; Li, G. *Eur. Polym. J* **2019**, *115*, 346-355.

(34) Tran, Y. H.; Rasmuson, M. J.; Emrick, T.; Klier, J.; Peyton, S. R. *Soft Matter* **2017**, *13* (47), 9007-9014.

(35) Mishra, D.; Wang, S.; Michel, S.; Palui, G.; Zhan, N.; Perng, W.; Jin, Z.; Mattoussi, H. *Phys. Chem. Chem. Phys.* **2018**, *20* (6), 3895-3902.

(36) Kisanuki, A.; Kimpara, Y.; Oikado, Y.; Kado, N.; Matsumoto, M.; Endo, K. *J. Polym. Sci.* **2010**, *48* (22), 5247-5253.

(37) Fairbanks, B. D.; Singh, S. P.; Bowman, C. N.; Anseth, K. S. *Macromolecules* **2011**, *44* (8), 2444-2450.

4.6 Supporting Information

4.6.1 Materials and instruments

Poly(ethylene glycol) (Mw 6 kDa) was obtained from Fluka, O-methyl-undecaethylene glycol (mPEG-11) from Polypure, **PEGdiSH** (6568 Da) from Iris, and **PEG4SH** (10 kDa) from Jenkem Technology. All other chemicals and reagents for synthesis were purchased from Sigma Aldrich and used without further purification. Deuterated water and chloroform were received from Euriso-top. Water was deionized before use. Dulbecco's phosphate buffered saline (DPBS) was purchased from Sigma-Aldrich. Dulbecco's modified Eagle medium (DMEM) was received from Gibco, Life Technologies. Propidium Iodide (PI) and calcein AM (AM = acetoxymethyl) were received from Sigma-Aldrich. µ-Slide 8 well plates were purchased from Ibidi. Polydimethylsiloxane (PDMS) (Sylgard 184 Silicon Elastomer Kit, Dow Corning), silicon wafer and fluorosilane (1H,1H,2H,2Hperfluorooctyltrichlorosilane) were purchased from VWR chemicals, Siegert Wafers and Sigma-Aldrich, respectively. Purification of **PEGmNB**, **PEGmDT** and the RGD-peptide was performed on a Grace Reveleris X1 flash chromatography system equipped with a C18 column, and subsequently by RP-HPLC on a Vydac C18 reverse-phase column with UV detection. ^{1}H-NMR and ^{13}C-NMR spectra of all the synthetic compounds were recorded at room temperature on a Bruker DMX-400 (400 MHz) operating at 400 MHz for ^{1}H-NMR and 100 MHz for ^{13}C-NMR. Solid-phase peptide synthesis was executed on a microwave-assisted Liberty Blue automated synthesizer from CEM (Matthews). LC-MS data were recorded on a Finnigan Surveyor HPLC system with Gemini C18 column (50 × 4.60 mm, UV detection: 200-600 nm) and also a Finnigan LCQ Advantage Max mass spectrometer with ESI. A solvent gradient of 10-90% of CH_3CN-H_2O (0.1% TFA) over 13.5 min was used for the mobile phase of the LC-MS. Oscillatory rheology experiments were performed on a Discovery Hybrid Rheometer (DHR-2, TA Instruments) using a 20 mm diameter parallel plate geometry with a UV curing accessory at room temperature. The Excelitas Omnicure S2000 system (λ = 320-500 nm, primary peak: 365 nm) with a light guide (5 mm diameter) was used as UV light source and connected to the rheology instrument. An anti-reflective chrome mask made of soda lime glass was obtained from Delta mask. Scanning electron micrographs were collected on a JSM-7600F microscope (JEOL) under a high vacuum with an acceleration voltage of 2.0 kV. Photopattering was performed in 3D using a Photonic Professional GT (Nanoscribe, Germany) with a

20x air objective (Zeiss, Germany). The 3D cell-laden hydrogels were imaged on a Zeiss LSM 710 confocal laser scanning microscope equipped with a Zeiss 5x objective. The photo-patterned hydrogels were imaged using a 10x objective on a Nikon Eclipse Ti microscope equipped with a Yokogawa confocal spinning disk unit operated at 10,000 rpm (Nikon).

4.6.2 Synthetic procedures

4-methyl-1,2-dithiolane-4-carboxylic acid, and **PEGdiNB** were synthesized as previously published.[1-3]

Synthesis of PEGdiDT

DCC (0.83 g, 4.0 mmol) was added to a stirred solution of 4-methyl-1,2-dithiolane-4-carboxylic acid (0.66 g, 4.0 mmol) in DCM (10 mL). A white precipitate was immediately observed after DCC addition. In a separate flask, poly(ethylene glycol) (Mw 6 kDa) (3.0 g, 0.5 mmol), pyridine (323 µL, 4.0 mmol) and DMAP (0.061 g, 0.5 mmol) were stirred at room temperature in DCM (10 mL). After 30 min, the two solutions were combined and further reacted at room temperature overnight. The mixed solution was filtered, and concentrated by a stream of nitrogen gas before being precipitated in cold diethyl ether, washed and re-dissolved in DCM. The precipitation step was repeated three times. The obtained solid was then re-dissolved in deionized water, dialyzed for two days and lyophilized overnight to obtain a white solid.

Yield: 2.64 g, 87%. ^{1}H-NMR (400 MHz, CDCl$_3$): 4.30-4.27 (m, 4H), 3.78-3.43 (m, 544H), 2.93-2.90 (d, 4H), 1.47 (s, 6H).

Synthesis of PEGmDT

O-Methyl-undecaethylene glycol (mPEG-11) (0.54 g, 1.04 mmol) was dissolved in DCM (15 mL), followed by the addition of 4-methyl-1,2-dithiolane-4-carboxylic acid (0.26 g, 1.57 mmol), 1-ethyl-3-(3- dimethylaminopropyl) carbodiimide (EDCI) (0.30 g, 1.65 mmol), and DMAP (0.026 g, 0.21 mmol). The reaction was stirred overnight at room temperature and the extent of reaction was determined by LC-MS prior to purification on a flash column chromatography system using a C18 silica gel column with a gradient of 10-90% CH$_3$CN/H$_2$O over 43 minutes. The product was concentrated by rotary evaporation and lyophilized overnight before

further purification by high performance liquid chromatography (HPLC) with UV detection. The purified product after lyophilization was a light yellow liquid.

Yield: 0.34 g, 49%. ^{1}H-NMR (CDCl$_3$, 400 MHz): 4.31-4.28 (m, 2H), 3.81-3.53 (m, 44H), 3.37 (s, 3H), 2.94-2.91 (d, 2H), 1.48 (s, 3H). LC-MS: t = 5.42 min, m/z calcd. for [M+H]$^+$: 664.30, found: 663.42 [M+H]$^+$.

Synthesis of PEGmNB

mPEG-11 (0.57 g, 1.11 mmol) was dissolved in DCM (15 mL), followed by the addition of 5-norbornene-2-carboxylic acid (203 µL, 1.67 mmol), EDCI (0.32 g, 1.67 mmol), and DMAP (0.027 g, 0.22 mmol). The reaction was allowed to stir overnight at room temperature and the extent of reaction was determined by LC-MS prior to purification on a flash column chromatography system using a C18 silica gel column with a gradient of 10-90% CH$_3$CN/H$_2$O over 43 minutes. The product was concentrated by rotary evaporation and lyophilized overnight before further purification on a HPLC by UV detection. The lyophilized product after purification was a colorless liquid.

Yield: 0.29 g, 41%. ^{1}H-NMR (CDCl$_3$, 400 MHz): 6.19-5.91 (m, 2H), 4.25-4.13 (m, 2H), 3.71-3.53 (m, 42H), 3.37 (s, 3H). LC-MS: t = 5.42-5.59 min, m/z calcd. for [M+H]$^+$: 637.37, found: 637.50 [M+H]$^+$.

Synthesis of (Fluorescein)GK(DT)GGGRGDS

(Fmoc)G-K(Mtt)-G-G-G-R(Pbf)-G-D(tBu)-S(tBu)-NH$_2$ was synthesized on a 0.1 mmol scale on a Rink Amide resin (Tentagel HL-RAM, loading capacity: 0.39 mmol g^{-1}). The Mtt protecting group was removed by washing several times with a deprotection solution of DCM:TFA:TIPS (94:1:5) at room temperature for 2 min until the solution became colorless to confirm the Mtt group was cleaved. The peptide was kept on resin and washed with DCM (3 x 3 mL) before coupling 4-methyl-1,2-dithiolane-4-carboxylic acid (82 mg, 0.5 mmol) to the free amine with HCTU (248 mg, 0.6 mmol) and DIPEA (174 µL, 1.0 mmol) in DMF (3 mL) with overnight shaking at room temperature. Subsequently, the Fmoc protecting group was removed with 20% piperidine in DMF with shaking at room temperature over 45 min, refreshing the cleavage solution every 15 min, followed by washing with DMF (3 x 3 mL). The N-terminal amine was then further coupled to 5(6)-carboxyfluorescein (188 mg, 0.5 mmol) with HCTU (248 mg, 0.6 mmol) and DIPEA

(174 μL, 1.0 mmol) in DMF (3 mL) on a shaker overnight at room temperature, followed by washing with 3 mL DMF and 3 mL DCM. Finally, a deprotection mixture of TFA:TIPS:water (95:2.5:2.5) was used to cleave the peptide from the resin by shaking at room temperature for 3h. The crude peptide was precipitated using cold diethyl ether, centrifuged, re-dissolved in water, and lyophilized overnight prior to purification by HPLC. A yellow solid was obtained after lyophilization and the product was confirmed by LC-MS: t = 4.62 min, calcd. for [M+H]$^+$: 1292.30, found: 1293.10 [M+H]$^+$. The peptide was stored at -20 °C in the dark before use.
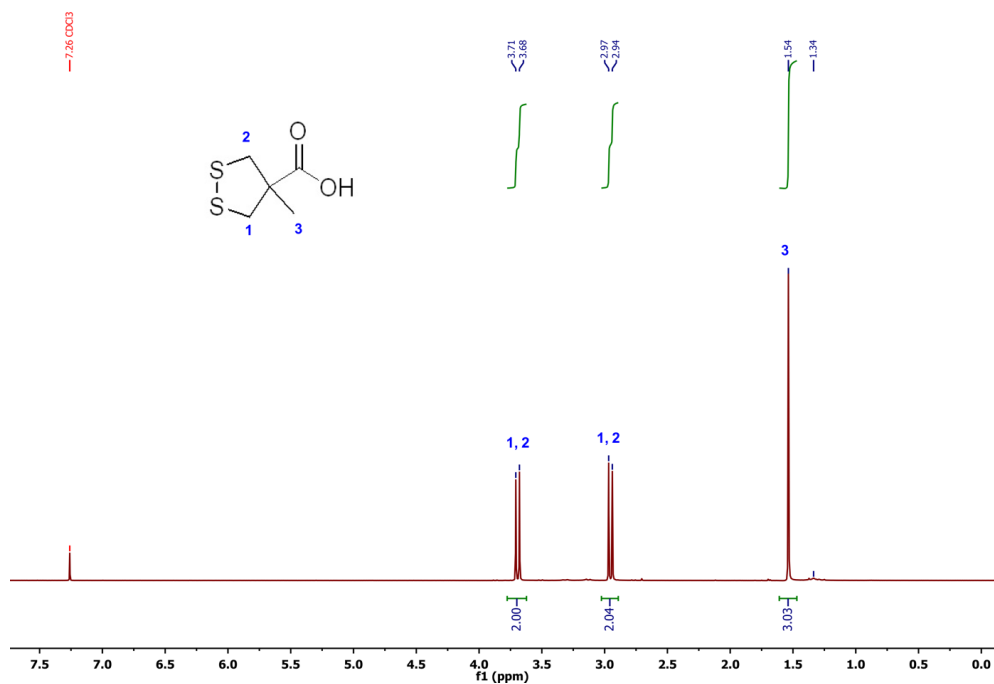
Figure S4.1 ^{1}H-NMR (400 MHz, 298 K, CDCl$_3$) spectrum of 4-methyl-1,2-dithiolane-4-carboxylic acid.
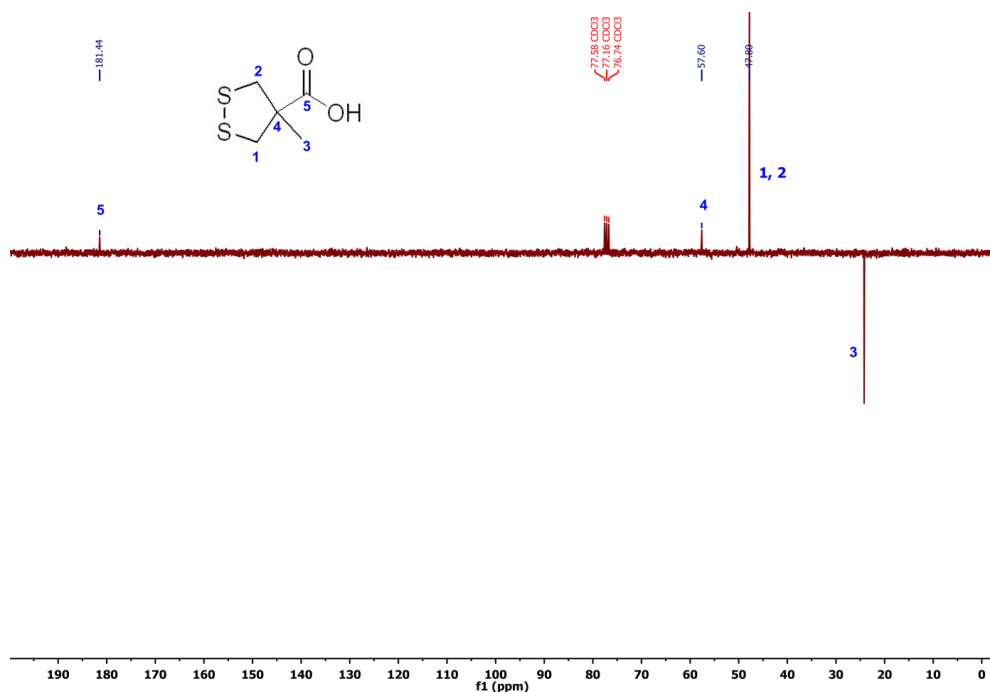
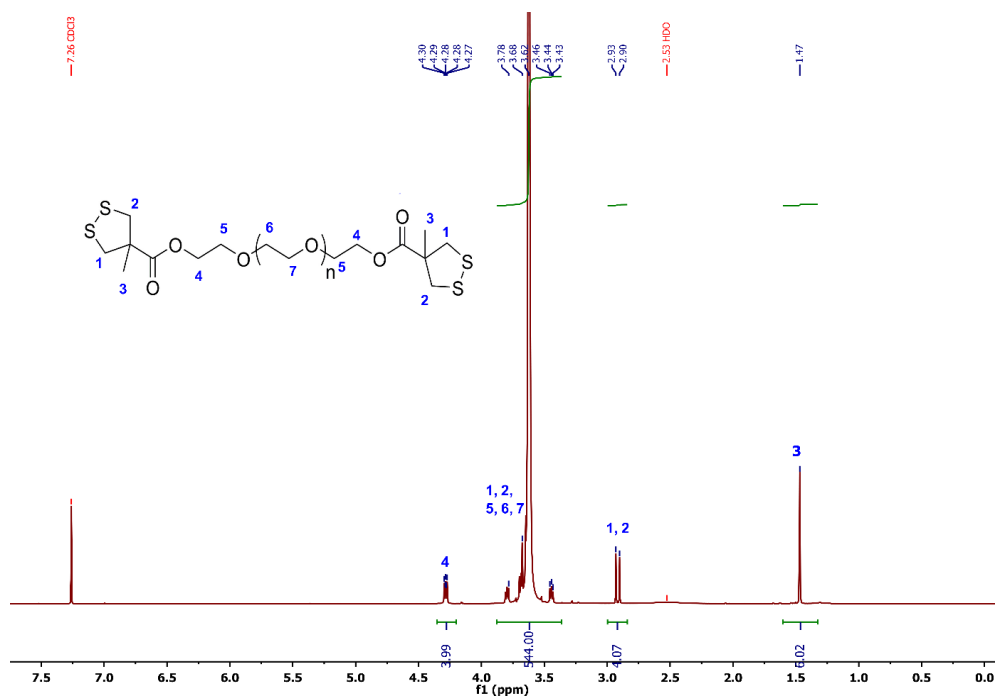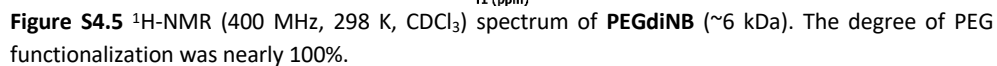**Figure S4.2** ^{13}C-NMR (100 MHz, 298 K, CDCl$_3$) spectrum of 4-methyl-1,2-dithiolane-4-carboxylic acid.
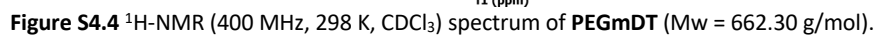

Figure S4.3 ^{1}H-NMR (400 MHz, 298 K, CDCl$_3$) spectrum of **PEGdiDT** (~6 kDa). The degree of functionalization was nearly 100%.

Figure S4.4 ^{1}H-NMR (400 MHz, 298 K, CDCl$_3$) spectrum of **PEGmDT** (Mw = 662.30 g/mol).

Figure S4.5 ^{1}H-NMR (400 MHz, 298 K, CDCl$_3$) spectrum of **PEGdiNB** (~6 kDa). The degree of PEG functionalization was nearly 100%.
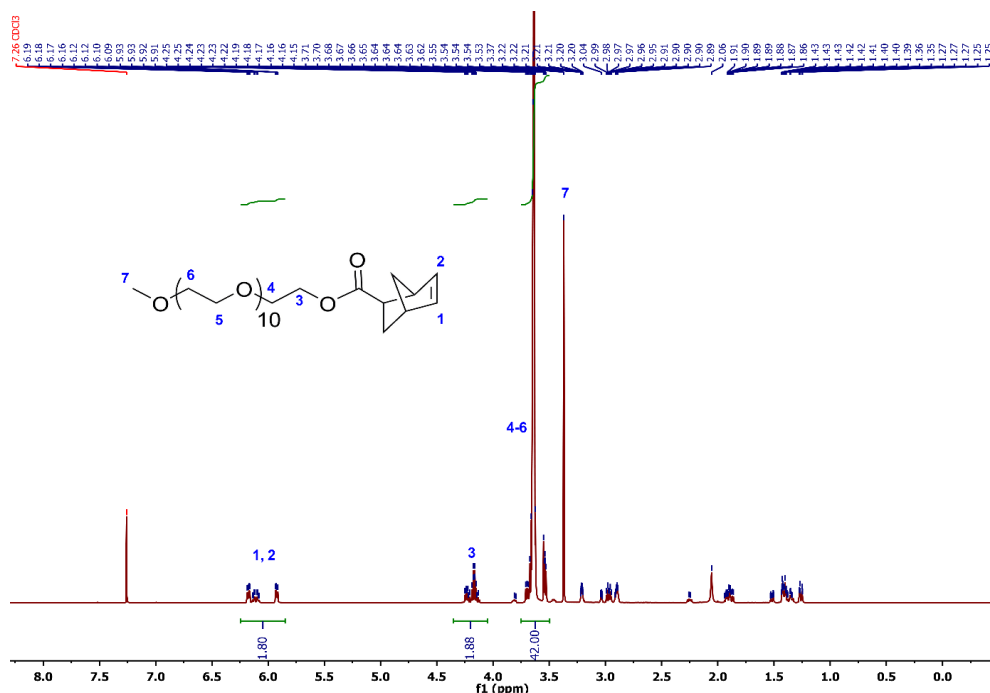
Figure S4.6 ^{1}H-NMR (400 MHz, 298 K, CDCl$_3$) spectrum of **PEGmNB** (Mw = 636.37 g/mol).

4.6.3 Hydrogel formation

A range of crosslinked polymer networks based on **PEGdiDT**, DT-NB (**PEGdiDT-PEGdiNB**) and SH-NB (**PEGdiSH-PEGdiNB**, **PEG4SH-PEGdiNB**) were prepared.

To form the **PEGdiDT** based hydrogels, **PEGdiDT** monomer was first weighed in a 2.0 mL vial and the required volume of PBS (pH 7.4) was added to obtain a homogeneous clear pre-gel solution after 30 s vortexing, followed by 30 min or 60 min UV irradiation through the Excelitas Omnicure S2000 system (~10 mW/cm^2, λ = 320-500 nm, primary peak: 365 nm) or a benchtop LED (~10 mW/cm^2, 375 nm).

To obtain the DT-NB based hydrogels (e.g., **PEGdiDT-PEGdiNB**), stock solutions of the complementary polymer precursors **PEGdiDT**, **PEGdiNB** and photoinitiator **LAP** were first prepared in PBS (pH 7.4) separately with vortexing for 30 s. Then, **PEGdiDT** (final concentration 1.0-8.0 mM) (70 µL), **PEGdiNB** (final concentration 1.0-8.0 mM) (70 µL), **LAP** (final concentration 0.1-4.0 mM) (10 µL) pipetted from their respective stock solutions were vortexed together for 30 s to obtain a homogeneous hydrogel precursor solution (150 µL) before mixing with the polymers containing the complementary reactive groups (at [NB]/[DT] molar ratios (2:1; 1:1; 1:2 and 1:3). The precursor solution was then irradiated with UV

light (from 5.0-30.0 mW/cm^2, λ = 320-500 nm, primary peak: 365 nm) at room temperature for 5-30 min to provide transparent hydrogels. The volume ratio of the **PEGdiNB**, **PEGdiDT** and **LAP** were always kept at 7:7:1. The preparation of **PEGdiSH-PEGdiNB** and **PEG4SH-PEGdiNB** samples followed the same procedure as above.
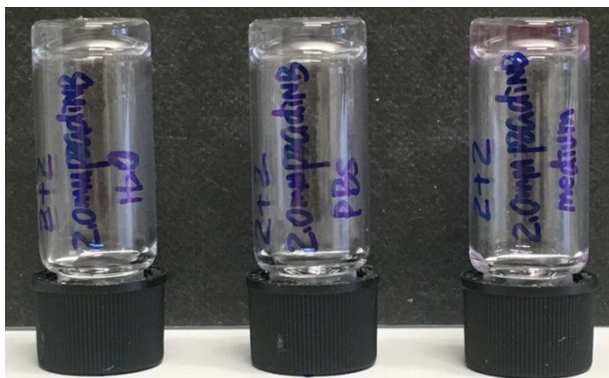

Figure S4.7 Gel inversion experiments of **PEGdiDT-PEGdiNB** hydrogels after 2 min UV irradiation using a benchtop LED (~10 mW/cm^2, 375 nm) at room temperature. 2.0 mM **PEGdiDT**-2.0 mM PEGdiNB-1.0 mM **LAP** in deionized water (*left*), in PBS (*middle*) and in cell culture media (DMEM) (*right*).

4.6.4 Rheology measurements

Pre-prepared PEG stock solutions (104 µL) were pipetted on a 20 mm PMMA plate directly and the gap was set to 300 mm. To trigger hydrogel formation, the UV light source (Excelitas Omnicure S2000 system, λ = 320-500 nm, primary peak: 365 nm) was turned on after data collection for 60 s. Time sweep measurements were carried out at 0.05% strain with a frequency (f) of 1.0 Hz. Frequency sweeps were recorded from 0.01 to 10 Hz at a constant strain of 0.05%. Strain sweeps were executed from 0.01 to 2000% with a frequency of 1.0 Hz. To measure the self-recovery of the hydrogels, a step-strain experiment was performed. First, a time sweep measurement was performed (f = 1.0 Hz, γ = 0.05%) with 5 min UV irradiation (~10 mW/cm^2, λ = 320-500 nm, primary peak: 365 nm) to reach the platform of the storage modulus (G'). Then a high strain of 1000% was applied for 300 s followed by the application of low strain 0.05% (f = 1.0 Hz) for another 300 s. The oscillation between high and low strain was repeated in this manner for two cycles.
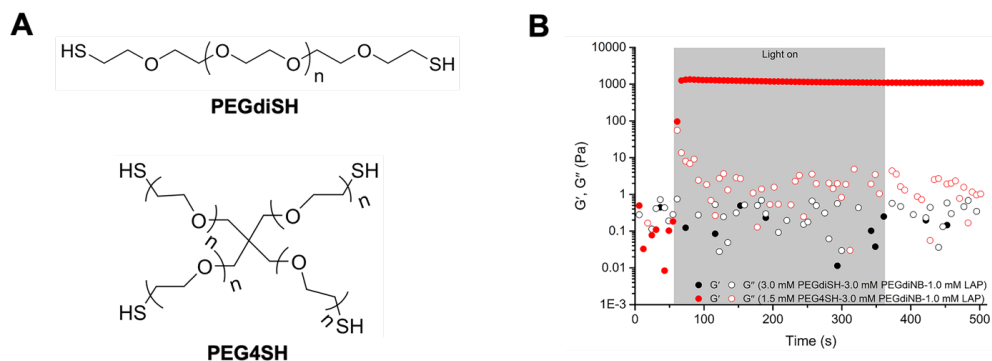
Figure S4.8 (A) Chemical structure of polymers **PEGdiSH** and **PEG4SH**. (B) Averaged (N = 3) time sweep data of SH-NB based hydrogels (3.0 mM **PEGdiSH**-3.0 mM **PEGdiNB**-1.0 mM **LAP**; and 1.5 mM **PEG4SH**-3.0 mM **PEGdiNB**-1.0 mM **LAP**) with 5 min UV irradiation. A constant strain (γ = 0.05%) and a fixed frequency (f = 1.0 Hz) were kept during the measurement at room temperature. The shaded part of the data indicates when light was applied.
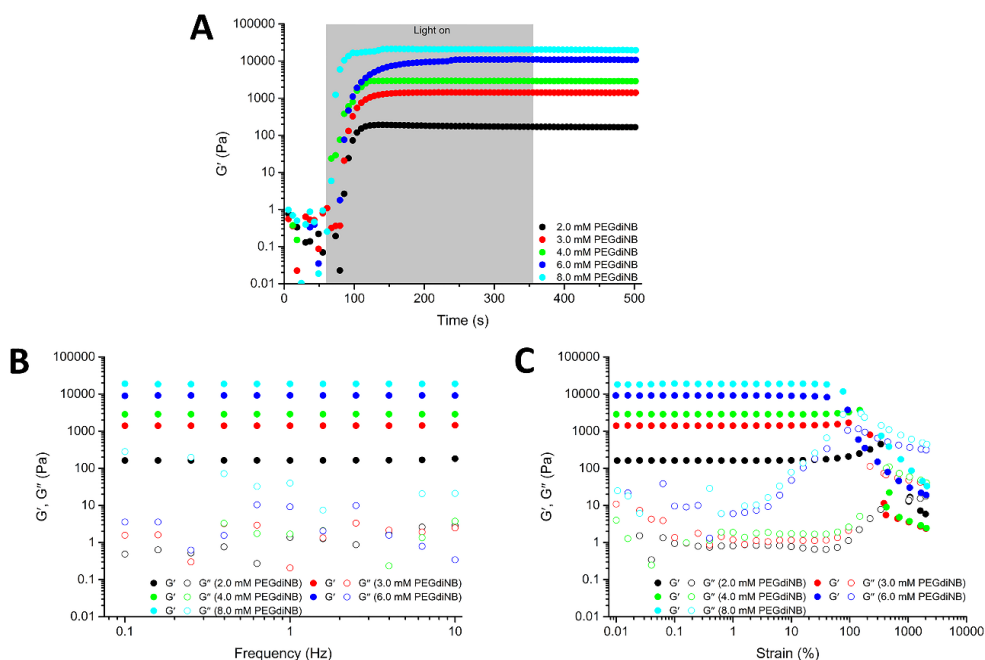

Figure S4.9 Averaged (N ≥ 3) time, frequency and strain sweeps of **PEGdiDT**-**PEGdiNB** hydrogels (molar ratio [NB]/[DT] = 1:1 and 1.0 mM **LAP**) with various monomer concentrations after UV irradiation (~10 mW/cm², λ = 320-500 nm, primary peak: 365 nm) for 5 min at room temperature: (A) Time sweep experiment at constant strain (γ = 0.05%) and frequency (f = 1.0 Hz); (B) Frequency sweep experiment at constant strain (γ = 0.05%); (B) Strain sweep experiment at a fixed frequency (f = 1.0 Hz). The shaded part of the data indicates when light was applied.
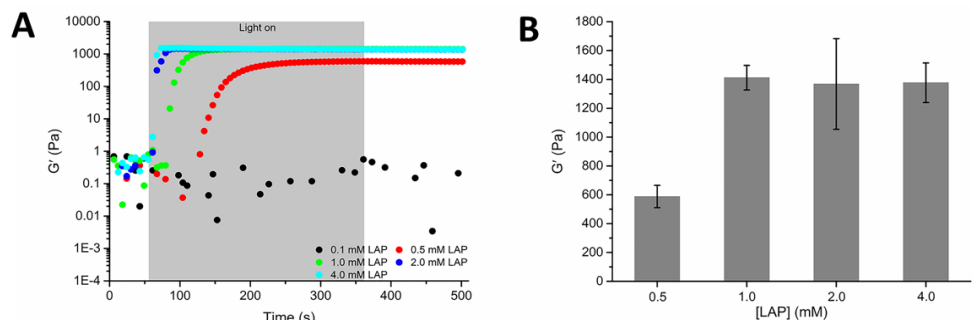
Figure S4.10 Averaged (N = 3) time sweep data (A) and plateau storage moduli (G') (B) of **PEGdiDT-PEGdiNB** system (3.0 mM **PEGdiDT**-3.0 mM **PEGdiNB**) using different photoinitiator **LAP** concentrations (0.1 mM, 0.5 mM, 1.0 mM, 2.0 mM and 4.0 mM) with UV irradiation (~10 mW/cm^2, λ = 320-500 nm, primary peak: 365 nm) for 5 min at room temperature. Error bars were determined according to the standard deviation of repeat measurements. The shaded part of the data indicates when light was applied.
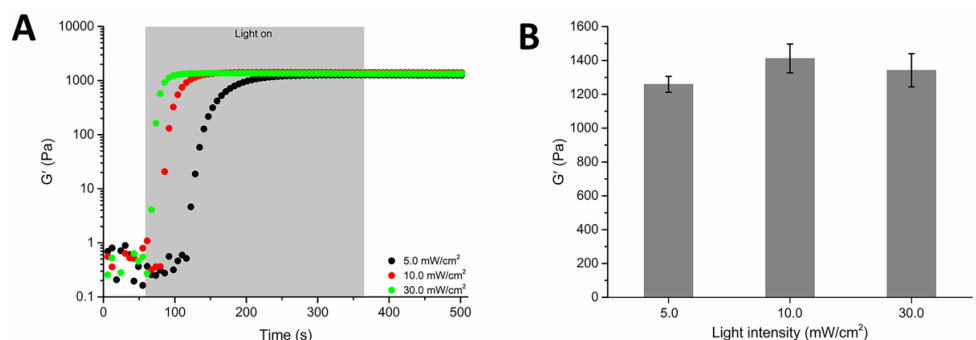

Figure S4.11 Averaged (N = 3) time sweep data (A) and plateau storage moduli (G') (B) of **PEGdiDT-PEGdiNB** hydrogels (3.0 mM **PEGdiDT**-3.0 mM **PEGdiNB**-1.0 mM **LAP**) with UV irradiation (λ = 320-500 nm, primary peak: 365 nm) with varied light intensity (~5.0 mW/cm^2, ~10 mW/cm^2 and ~30 mW/cm^2) for 5 min. Error bars were determined according to the standard deviation of repeat measurements. The shaded part of the data indicates when light was applied.
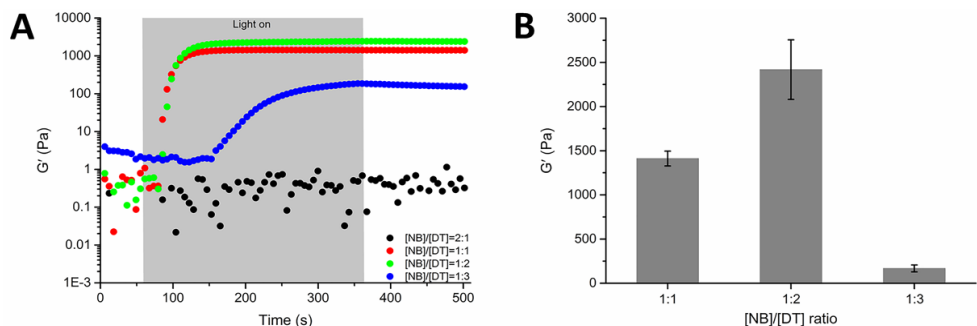
Figure S4.12 Averaged (N = 3) time sweep data (A) and plateau storage moduli (G') (B) **PEGdiDT**-**PEGdiNB** hydrogels using 3.0 mM **PEGdiNB** and 1.0 mM **LAP** with various molar ratios of [NB]/[DT] (2:1; 1:1; 1:2; 1:3) under UV irradiation (~10 mW/cm^2, λ = 320-500 nm, primary peak: 365 nm) for 5 min. Error bars were calculated according to the standard deviation of repeat measurements. The shaded part of the data indicates when light was applied.
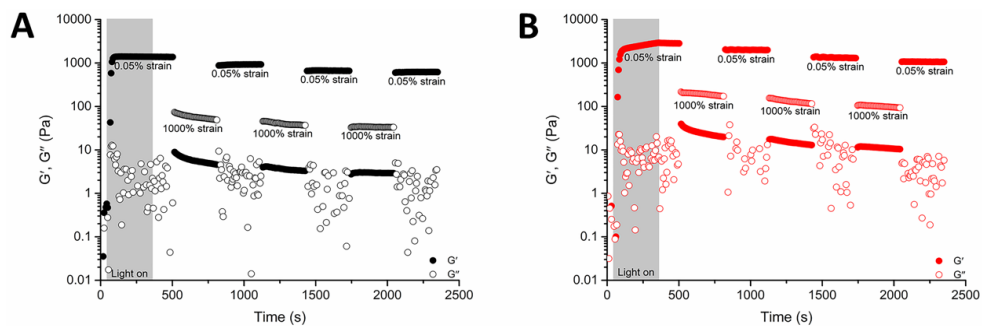

Figure S4.13 Averaged (N = 3) step-strain measurements of **PEGdiDT**-**PEGdiNB** hydrogels with different [NB]/[DT] molar ratios after UV irradiation (~10 mW/cm^2, λ = 320-500 nm, primary peak: 365 nm) for 5 min: (A) 3.0 mM **PEGdiDT**-3.0 mM **PEGdiNB**-1.0 mM **LAP** ([NB]/[DT] = 1:1); (B) 6.0 mM **PEGdiDT**-3.0 mM **PEGdiNB**-1.0 mM **LAP** ([NB]/[DT] = 1:2). The shaded part of the data indicates when light was applied.

Table S4.1 Gelation behaviors and plateau storage moduli (G') of the various polymer precursors with different UV light source parameters (λ = 320-500 nm, primary peak: 365 nm). Averaged G' values are presented (N ≥ 3).

PEGdiDT (mM)	PEGdiSH (mM)	PEG4SH (mM)	PEGdiNB (mM)	LAP (mM)	Light intensity (mW/cm^2)	Irradiation time (min)	G' (Pa)
6.0	-	-	-	-	10	30	42 ± 6
6.0	-	-	-	1.0	10	30	No gel
6.0	-	-	-	-	10	60	181 ± 18
12.0	-	-	-	-	10	60	895 ± 158
3.0	-	-	3.0	-	10	30	No gel
3.0	-	-	3.0	1.0	10	30	1265 ± 62
-	3.0	-	3.0	1.0	10	5	No gel
-	-	1.5	3.0	1.0	10	5	1095 ± 17
-	-	3.0	3.0	1.0	10	5	146 ± 31
1.0	-	-	1.0	1.0	10	5	No gel
2.0	-	-	2.0	1.0	10	5	167 ± 11
3.0	-	-	3.0	1.0	10	5	1412 ± 84
4.0	-	-	4.0	1.0	10	5	2898 ± 45
6.0	-	-	6.0	1.0	10	5	10882 ± 2444
8.0	-	-	8.0	1.0	10	5	20018 ± 1751
3.0	-	-	3.0	0.1	10	5	No gel
3.0	-	-	3.0	0.5	10	5	588 ± 77
3.0	-	-	3.0	2.0	10	5	1368 ± 314
3.0	-	-	3.0	4.0	10	5	1377 ± 137
3.0	-	-	3.0	1.0	5	5	1259 ± 47
3.0	-	-	3.0	1.0	30	5	1342 ± 98
1.5	-	-	3.0	1.0	10	5	No gel
6.0	-	-	3.0	1.0	10	5	2418 ± 337
9.0	-	-	3.0	1.0	10	5	168 ± 39

4.6.5 Scanning electron microscopy (SEM)

The hydrogel 2.0 mM **PEGdiDT**-2.0 mM **PEGdiNB**-1.0 mM **LAP** was prepared according to the above gelation protocol and lyophilized overnight. The dried hydrogel sample was then applied to two-sided adhesive tape before being attached to an aluminum stub. The samples were sputtered for 2 min with a thin layer of gold prior to imaging.
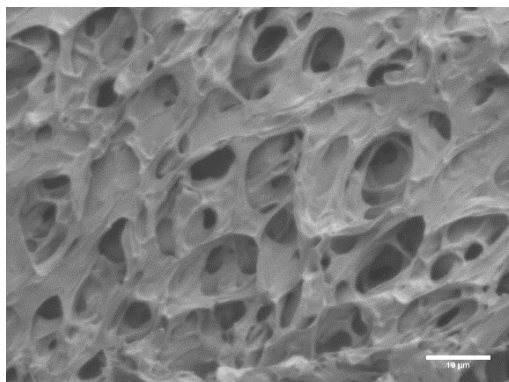
Figure S4.14 SEM images of a freeze-dried hydrogel of **PEGdiDT**-**PEGdiNB** (2.0 mM **PEGdiDT**-2.0 mM **PEGdiNB**-1.0 mM **LAP**) after UV irradiation for 5 min using a benchtop LED (~10 mW/cm², 375 nm). Scale bar: *10 μm.*

4.6.6 Swelling and degradation assays

The hydrogel swelling ratios were determined according to a previously published method.[4] Individual pregelation solutions in PBS (150 µL), e.g., 12.0 mM **PEGdiDT**, 3.0 mM **PEGdiDT**-3.0 mM **PEGdiNB**-1.0 mM **LAP**, and 6.0 mM **PEGdiDT**-3.0 mM **PEGdiNB**-1.0 mM **LAP**, were first prepared in 2.0 mL vial. The pre-gel solutions of **PEGdiDT** and **PEGdiDT-PEGdiNB** were UV irradiated for 60 and 5 min, respectively, using a benchtop of LED (~10 mW/cm², 375 nm) to enable gel formation. Each hydrogel was washed once with PBS (500 µL) before collecting the original gel weight (W_0). Subsequently, each hydrogel was covered with PBS (pH 7.4) or cell culture medium (DMEM) (800 µL), and incubated at 37 °C. The weight (W_t) of the various hydrogels were then collected at predetermined time points after removal of PBS or DMEM from the hydrogel surface. The swelling ratio was determined as W_t/W_0. For each sample condition, three replicates were performed.
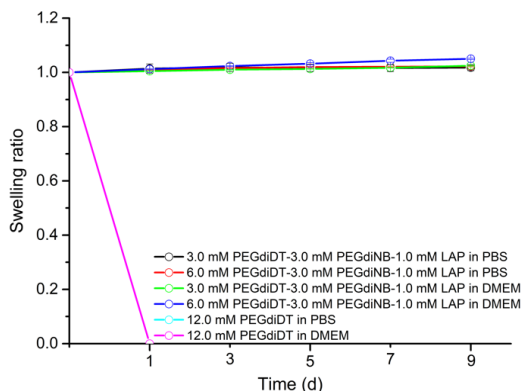
Figure S4.15 Average (N = 3) swelling ratios of **PEGdiDT** and **PEGdiDT**-**PEGdiNB** formed by irradiation with UV light for 60 and 5 min, respectively, using a benchtop LED (~10 mW/cm², 375 nm). Swelling rations were determined for the hydrogels at different time points in PBS and DMEM at 37 °C. Error bars were calculated according to the standard deviation of repeat measurements.

4.6.7 ¹H-NMR measurements

Solutions (A) 20.0 mM **PEGmDT**, (B) 20.0 mM **PEGmDT**-1.0 mM **LAP**, (C) 20.0 mM **PEGmDT**-10.0 mM **LAP**, (D) 20.0 mM **PEGmNB**, (E) 20.0 mM **PEGmNB**-1.0 mM **LAP**, (F) 20.0 mM **PEGmNB**-10.0 mM **LAP**, (G) 1.0 mM **LAP**, (H) 10.0 mM **PEGmDT**-10.0 mM **PEGmNB** ([NB]/[DT] = 1:1) different **LAP** concentrations (0 mM, 0.1 mM, 0.5 mM, and 1.0 mM), (I) 5.0 mM **PEGmDT**-10.0 mM **PEGmNB**-1.0 mM **LAP** ([NB]/[DT] = 2:1), and (J) 20.0 mM **PEGmDT**-10.0 mM **PEGmNB**-1.0 mM **LAP** ([NB]/[DT] = 1:2), were individually prepared in D₂O (1650 µL) in a 2 mL glass vial. Each solution was split into three by pipetting an aliquot of each solution (550 µL) into three separate vials (2 mL) for subsequent UV light irradiation at three-time intervals (0 min, 5 min and 30 min) using a benchtop LED source at 375 nm (~10 mW/cm²). The irradiated solutions (550 µL) were then transferred into an NMR tube and measured by ¹H-NMR spectroscopy. For each sample condition, at least two individual experiments were performed.
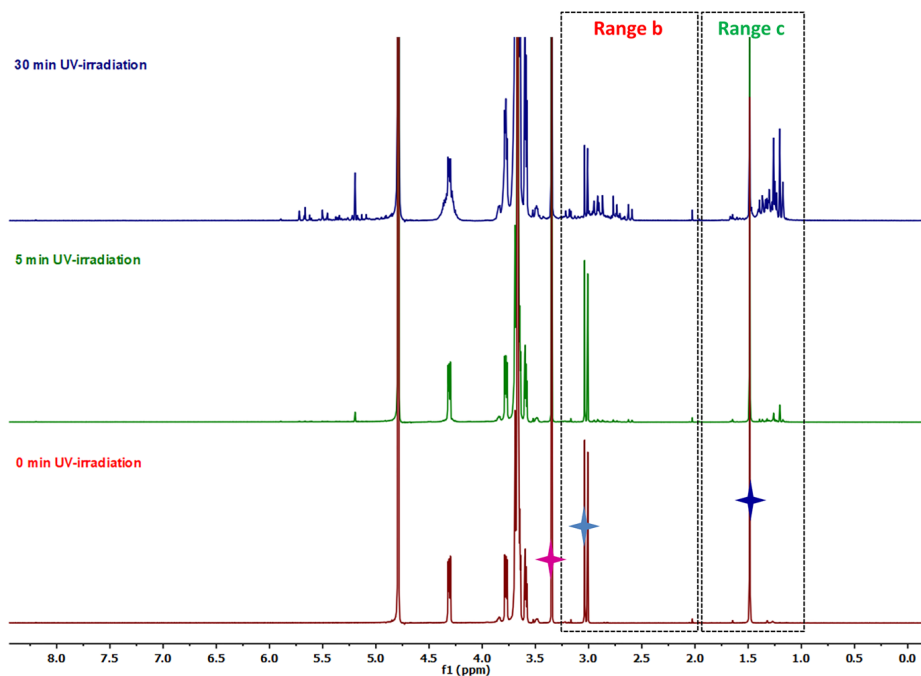
Figure S4.16 ^{1}H-NMR (400 MHz, 298 K) of 20.0 mM **PEGmDT** in D$_2$O with different UV irradiation times using a benchtop LED (~10 mW/cm^2, 375 nm): 0 min (*red line*), 5 min (*green line*), and 30 min (*blue line*).
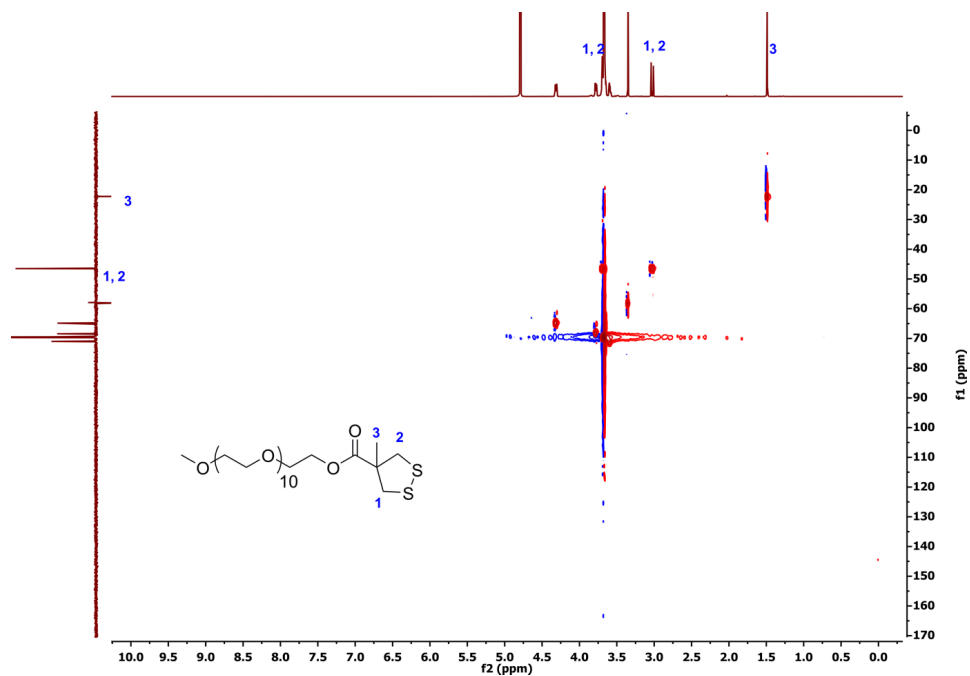

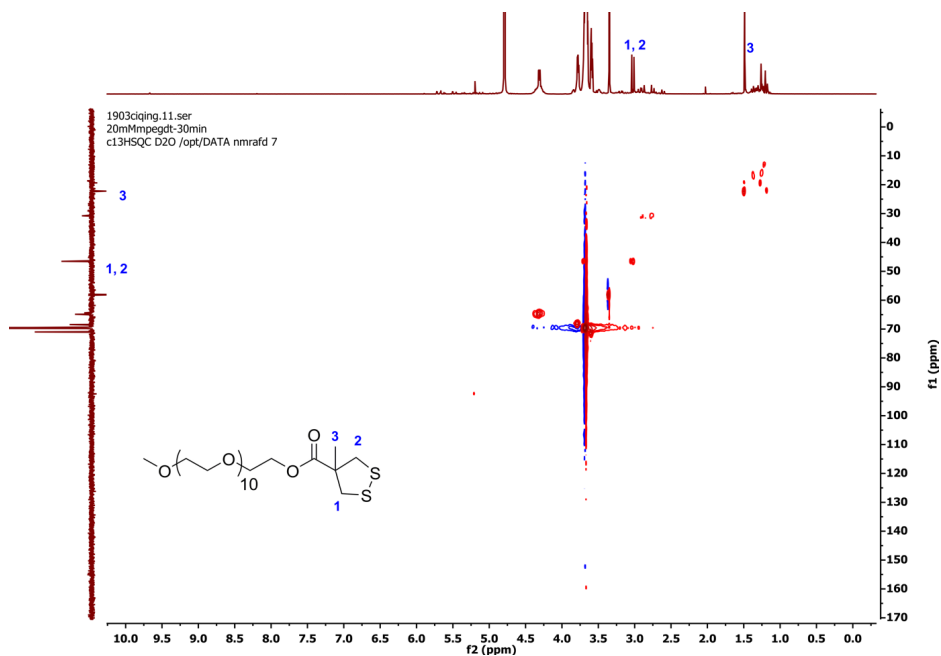**Figure S4.17** HSQC of 20.0 mM **PEGmDT** in D$_2$O without UV irradiation.

Figure S4.18 HSQC of 20.0 mM **PEGmDT** in D_2O with 30 min UV irradiation using a benchtop LED (~10 mW/cm^2, 375 nm).

Figure S4.19 ^{1}H-NMR (400 MHz, 298 K) of 20.0 mM **PEGmDT** with 1.0 mM **LAP** in D_2O with different UV irradiation times using a benchtop LED (~10 mW/cm^2, 375 nm): 0 min (*red line*), 5 min (*green line*), and 30 min (*blue line*).

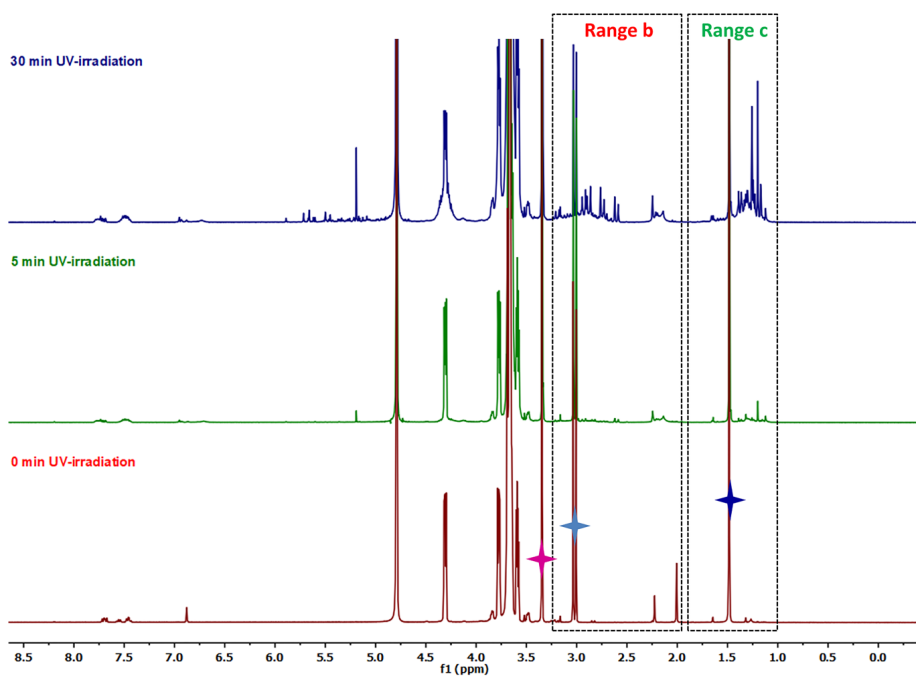**Figure S4.20** ^{1}H-NMR (400 MHz, 298 K) of 20.0 mM **PEGmDT** with 10.0 mM **LAP** in D$_2$O with different UV irradiation times using a benchtop LED (~10 mW/cm², 375 nm): 0 min (*red line*), 5 min (*green line*), and 30 min (*blue line*).

Figure S4.21 ^{1}H-NMR (400 MHz, 298 K) of 20.0 mM **PEGmNB** in D$_2$O with different UV irradiation times using a benchtop LED (~10 mW/cm^2, 375 nm): 0 min (*red line*), 5 min (*green line*), and 30 min (*blue line*).
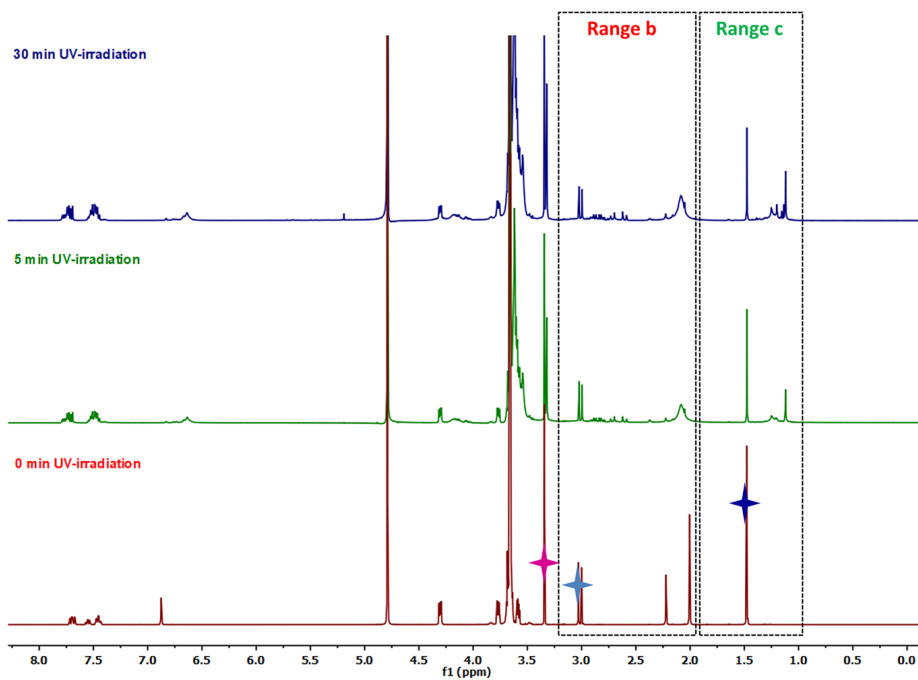
Figure S4.22 ^{1}H-NMR (400 MHz, 298 K) of 20.0 mM **PEGmNB** with 1.0 mM **LAP** in D$_2$O with different UV irradiation times using a benchtop LED (~10 mW/cm^2, 375 nm): 0 min (*red line*), 5 min (*green line*), and 30 min (*blue line*).

Figure S4.23 ^{1}H-NMR (400 MHz, 298 K) of 20.0 mM **PEGmNB** with 10.0 mM **LAP** in D$_2$O with different UV irradiation times using a benchtop LED (~10 mW/cm^2, 375 nm): 0 min (*red line*), 5 min (*green line*), and 30 min (*blue line*).

Figure S4.24 ^{1}H-NMR (400 MHz, 298 K) of 1.0 mM **LAP** in D$_2$O with different UV irradiation time using a benchtop LED (~10 mW/cm^2, 375 nm): 0 min (*red line*), 5 min (*green line*), and 30 min (*blue line*).
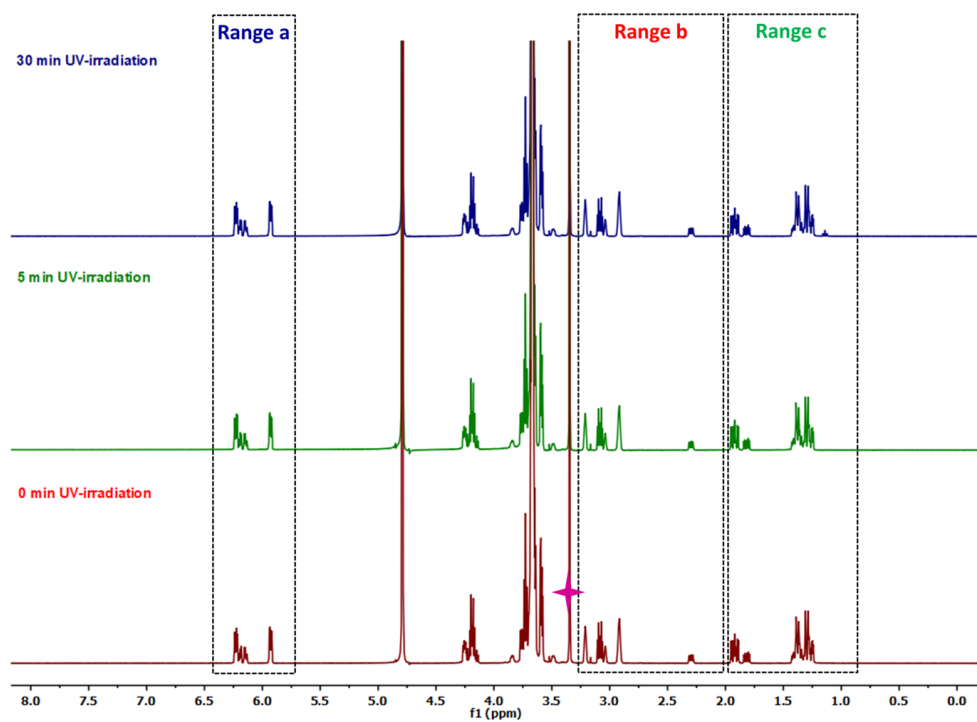
Figure S4.25 ^{1}H-NMR (400 MHz, 298 K) of 10.0 mM **PEGmDT**-10.0 mM **PEGmNB** ([NB]/[DT] = 1:1) with 1.0 mM **LAP** in D$_2$O with different UV irradiation time using a benchtop LED (~10 mW/cm^2, 375 nm): 0 min (*red line*), 5 min (*green line*), and 30 min (*blue line*).

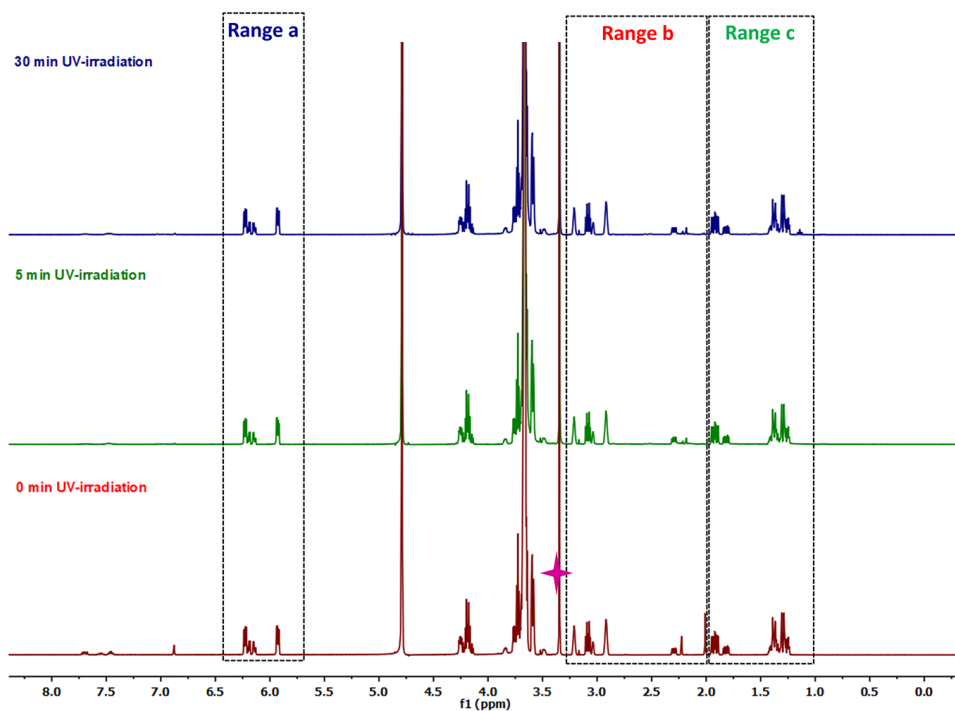**Figure S4.26** ^{1}H-NMR (400 MHz, 298 K) of 5.0 mM **PEGmDT**-10.0 mM **PEGmNB** ([NB]/[DT] = 2:1) with 1.0 mM **LAP** in D$_2$O with different UV irradiation time using a benchtop LED (~10 mW/cm^2, 375 nm): 0 min (*red line*), 5 min (*green line*), and 30 min (*blue line*).

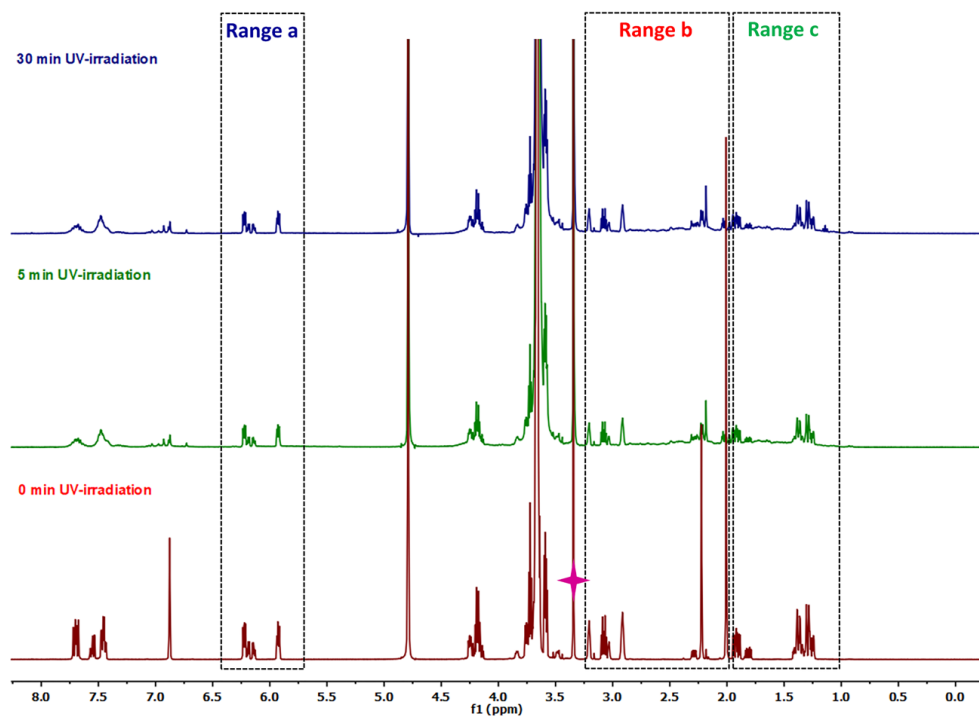**Figure S4.27** ^{1}H-NMR (400 MHz, 298 K) of 20.0 mM **PEGmDT**-10.0 mM **PEGmNB** ([NB]/[DT] = 1:2) with 1.0 mM **LAP** in D_2O with different UV irradiation time using a benchtop LED (~10 mW/cm^2, 375 nm): 0 min (*red line*), 5 min (*green line*), and 30 min (*blue line*).

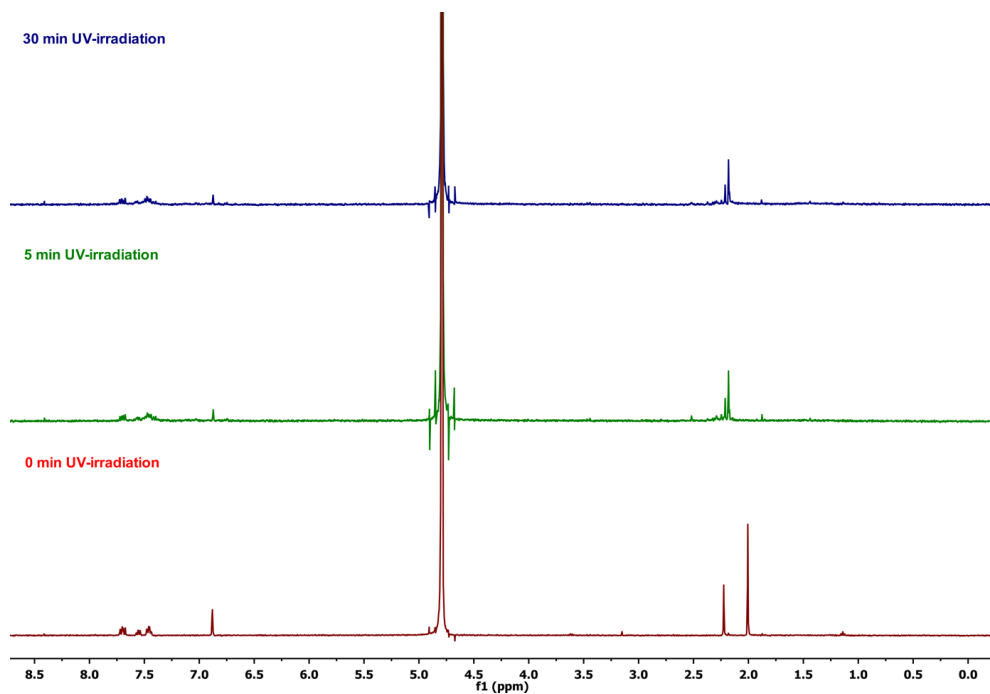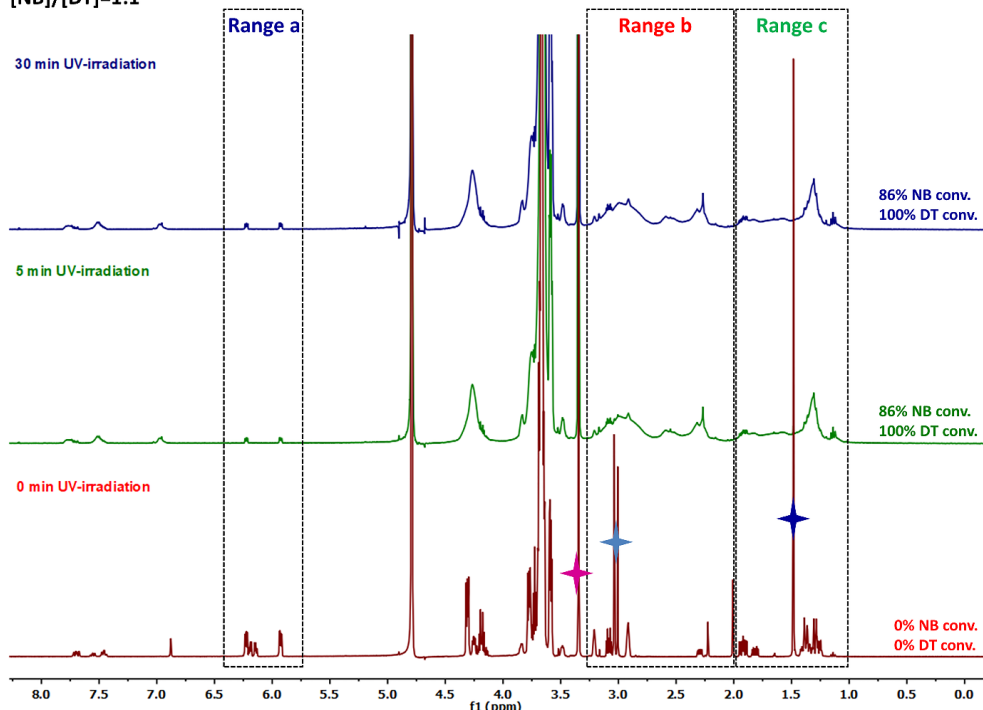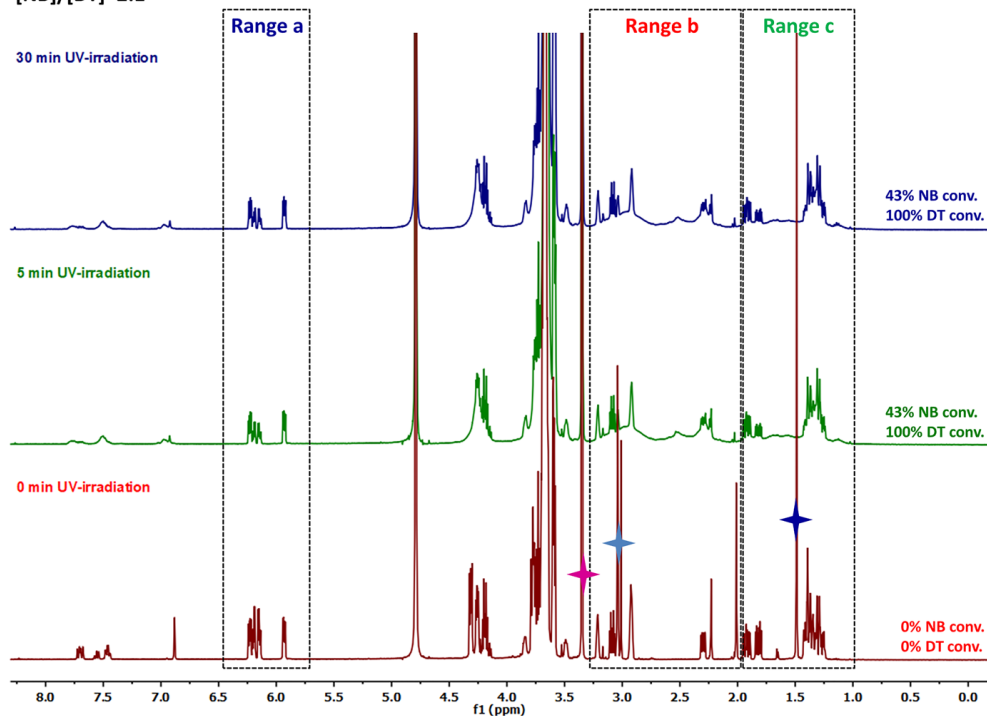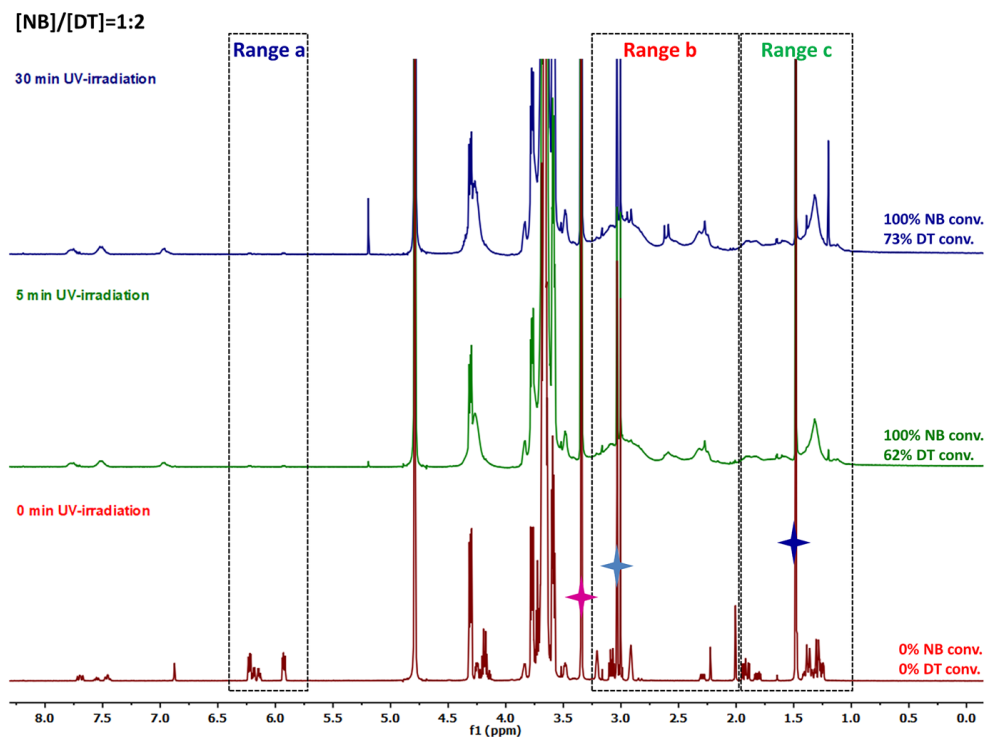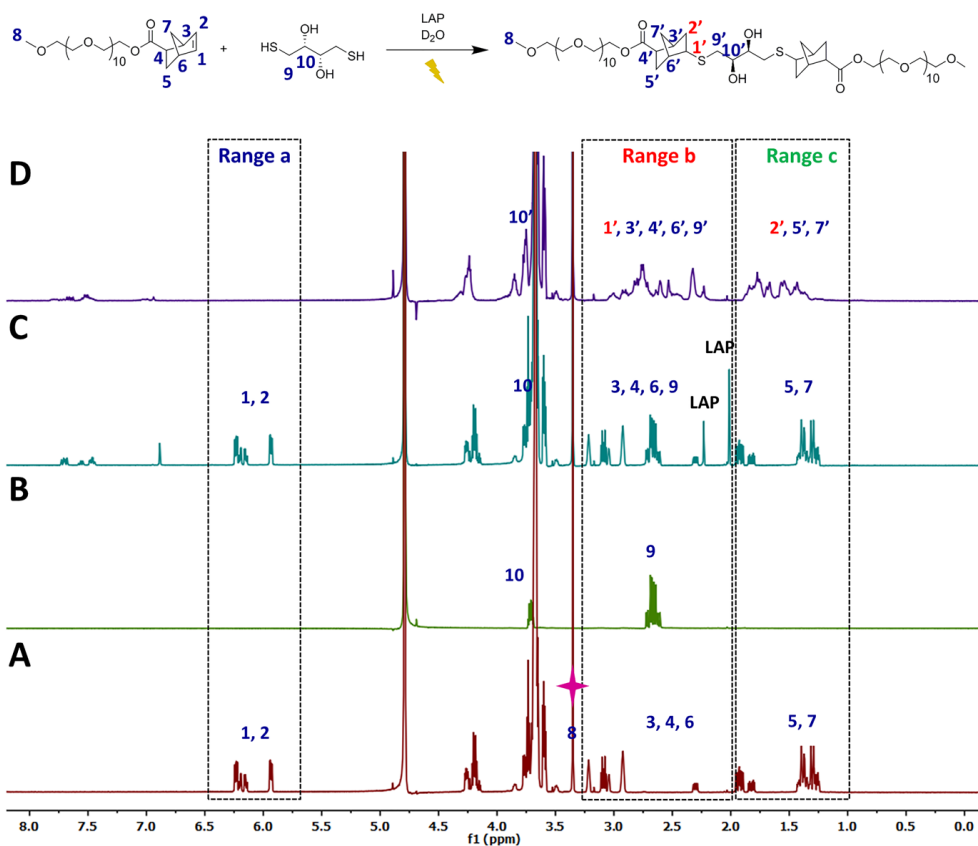**Figure S4.28** ^{1}H-NMR (400 MHz, 298 K) of (A) 10.0 mM **PEGmNB**; (B) 5.0 mM **DTT**; (C) 5.0 mM **DTT**-10.0 mM **PEGmNB**-1.0 mM **LAP** ([NB]/[SH] = 1:1) without UV irradiation and (D) 5.0 mM **DTT**-10.0 mM **PEGmNB**-1.0 mM **LAP** ([NB]/[SH] = 1:1) in D_2O with 5 min UV irradiation time using a benchtop LED (~10 mW/cm², 375 nm).

Table S4.2 Integrated areas and estimated conversion from ^{1}H-NMR spectrum of **PEGmDT** without and with different concentrations of **LAP** at various UV irradiation times using a benchtop LED (~10 mW/cm², 375 nm).

PEGmDT (mM)	LAP (mM)	UV time (min)	$A_{\sim3.35\ ppm}$ (a. u.)	$A_{\sim3.04-3.01\ ppm}$ (a. u.)	$A_{\sim1.49\ ppm}$ (a. u.)	$A_{range\ b}$ (a. u.)	$A_{range\ c}$ (a. u.)	DT conv. (%)
20.0	0	0	3	2.03	3.08	2.03	3.18	0
20.0	0	5	3	1.68	2.57	2.12	3.25	16
20.0	0	30	3	0.43	0.75	2.62	3.46	76
20.0	1.0	0	3	2.02	3.05	2.47	3.08	0
20.0	1.0	5	3	1.73	2.53	2.58	3.10	17
20.0	1.0	30	3	0.62	0.92	2.61	3.11	70
20.0	10.0	0	3	2.04	3.06	6.67	3.07	0
20.0	10.0	5	3	0.76	0.87	6.44	3.03	72
20.0	10.0	30	3	0.61	0.63	6.01	3.23	79

Range b: 1.99-3.30 ppm; range c: 1.00-1.98 ppm.

Table S4.3 Integrated areas and estimated conversion from ^{1}H-NMR spectrum of **PEGmNB** with various **LAP** concentrations under different UV irradiation times using a benchtop LED (~10 mW/cm^2, 375 nm).

PEGmNB (mM)	LAP (mM)	UV time (min)	$A_{\sim3.35\ ppm}$ (a. u.)	$A_{range\ a}$ (a. u.)	$A_{range\ b}$ (a. u.)	$A_{range\ c}$ (a. u.)	NB conv. (%)
20.0	0	0	3	2.02	3.20	4.20	0
20.0	0	5	3	2.12	2.62	4.02	0
20.0	0	30	3	2.09	3.10	4.20	0
20.0	1.0	0	3	2.04	3.29	4.06	0
20.0	1.0	5	3	1.97	3.84	4.58	3
20.0	1.0	30	3	1.84	3.23	4.14	10
20.0	10.0	0	3	1.91	7.44	4.19	0
20.0	10.0	5	3	1.01	5.22	4.33	47
20.0	10.0	30	3	1.15	5.83	4.91	40

Range a: 5.92-6.24 ppm (-ene of norbornene unit); range b: 1.99-3.30 ppm; range c: 1.00-1.98 ppm.

Table S4.4 Integrated areas and estimated conversion from ^{1}H-NMR spectrum of the DT-NB reaction (**PEGmDT-PEGmNB**) with different UV irradiation times using a benchtop LED (~10 mW/cm^2, 375 nm).

PEGmDT (mM)	PEGmNB (mM)	LAP (mM)	UV time (min)	$A_{\sim3.35\ ppm}$ (a. u.)	$A_{\sim1.49\ ppm}$ (a. u.)	$A_{range\ a}$ (a. u.)	$A_{range\ b}$ (a. u.)	$A_{range\ c}$ (a. u.)	DT conv. (%)	NB conv. (%)
5.0	10 (N = 1)	1.0	0	9	2.94	3.92	10.09	11.49	0	0
5.0	10 (N = 1)	1.0	5	9	0	2.24	13.72	11.25	100	43
5.0	10 (N = 1)	1.0	30	9	0	2.24	13.69	11.20	100	43
5.0	10 (N = 2)	1.0	0	9	2.96	4.02	9.0	10.74	0	0
5.0	10 (N = 2)	1.0	5	9	0	2.49	15.07	12.06	100	38
5.0	10 (N = 2)	1.0	30	9	0	2.48	14.45	11.74	100	38
10.0	10 (N = 1)	1.0	0	6	3.05	2.17	6.25	7.70	0	0
10.0	10 (N = 1)	1.0	5	6	0	0.27	9.83	6.90	100	86
10.0	10 (N = 1)	1.0	30	6	0	0.33	9.93	7.14	100	86
10.0	10 (N = 2)	1.0	0	6	2.91	2.26	7.30	7.92	0	0
10.0	10 (N = 2)	1.0	5	6	0	0.54	10.61	7.29	100	76
10.0	10 (N = 2)	1.0	30	6	0	0.51	10.40	7.25	100	77
10.0	10 (N = 1)	0	0	6	2.99	2.15	6.25	7.86	0	0
10.0	10 (N = 1)	0	5	6	2.71	2.16	5.95	7.79	9	0
10.0	10 (N = 1)	0.5	5	6	0.31	0.72	10.85	7.65	90	67
10.0	10 (N = 1)	1.0	5	6	0.13	0.56	11.09	7.59	96	74
10.0	10 (N = 2)	0.1	5	6	2.35	2.16	6.89	8.07	19	3
10.0	10 (N = 2)	0.5	5	6	0	0.59	11.17	7.50	89	71
10.0	10 (N = 2)	1.0	5	6	0	0.47	10.28	7.15	100	80
10.0	10 (N = 3)	0	0	6	2.91	2.27	6.24	7.81	0	0
10.0	10 (N = 3)	0.1	5	6	2.56	1.90	6.22	7.55	12	16
10.0	10 (N = 3)	0.5	5	6	0.39	0.75	10.42	7.51	86	67
10.0	10 (N = 3)	1.0	5	6	0	0.48	10.05	6.99	100	80
20.0	10 (N = 1)	1.0	0	9	6.02	1.87	7.26	10.06	0	0
20.0	10 (N = 1)	1.0	5	9	1.76	0	14.96	11.06	71	100
20.0	10 (N = 1)	1.0	30	9	0.73	0	14.15	10.78	88	100
20.0	10 (N = 2)	1.0	0	9	5.91	1.95	8.51	10.40	0	0
20.0	10 (N = 2)	1.0	5	9	2.22	0	14.69	10.76	62	100
20.0	10 (N = 2)	1.0	30	9	1.61	0	14.31	10.37	73	100

Range a: 5.92-6.24 ppm (-ene of norbornene unit); range b: 1.99-3.30 ppm; range c: 1.00-1.98 ppm.

Table S4.5 Integrated areas and estimated conversion in ¹H-NMR spectrum of the SH-NB reaction (**DTT-PEGmNB**) with different UV irradiation times using a benchtop LED (~10 mW/cm², 375 nm).

DTT (mM)	PEGmNB (mM)	LAP (mM)	UV time (min)	A~3.35 ppm (a. u.)	A range a (a. u.)	A range b (a. u.)	A range c (a. u.)	SH conv. (%)	NB conv. (%)
5.0	10.0 (N=1)	1.0	0	6	3.94	11.93	8.05	0	0
5.0	10.0 (N=1)	1.0	5	6	0	14.67	10.76	100	100
5.0	10.0 (N=1)	1.0	30	6	0	15.04	11.10	100	100
5.0	10.0 (N=2)	1.0	0	6	4.09	11.51	7.83	0	0
5.0	10.0 (N=2)	1.0	5	6	0	15.08	11.47	100	100

Range a: 5.92-6.24 ppm (-ene of norbornene unit); range b: 1.99-3.30 ppm; range c: 1.00-1.98 ppm.

4.6.8 3D cell encapsulation and cell viability

NIH 3T3 cells were cultured and maintained in DMEM medium with 10% FBS, penicillin (100 units/mL) and streptomycin (100 µg/mL) in an incubator at 37 °C with a 5% CO_2 atmosphere.

3D cell encapsulation in the **PEGdiDT-PEGdiNB** hydrogel was performed as follows: cells were trypsinized, centrifuged and re-suspended in cell culture medium. A cell suspension (20 µL, 3.6×10^6 cells/mL) was mixed with PEG pre-prepared precursor gel solutions (130 µL) by gently pipetting up and down (~10 times) to obtain a homogeneous cell-polymer suspension at the desired polymer concentrations (e.g., 2.0 mM **PEGdiDT**-2.0 mM **PEGdiNB**-1.0 mM **LAP** and 3.0 mM **PEGdiDT**-3.0 mM **PEGdiNB**-1.0 mM **LAP**). The cell-polymer suspension (150 µL) was pipetted into an 8-well chamber slide and irradiated with UV light for 2 min using a benchtop LED source (~10 mW/cm², 375 nm) to provide transparent 3D cell-laden hydrogels. Cell culture media (150 µL) was layered on top of the hydrogels and cultured in an incubator at 37 °C with a 5% CO_2 atmosphere. The cell media was refreshed daily for the duration of the experiment.

Cell viability was evaluated at pre-determined time points (e.g., 24 h and 48 h) by the LIVE/DEAD (calcein AM/propidium iodide (PI)) assay. Pre-prepared stock solutions of calcein AM (2.5 mM in DMSO) and PI (1.5 mM in PBS) were diluted with PBS (pH 7.4) to obtain a final staining solution containing calcein AM (2.0 µM) and PI (1.5 µM). The medium was first removed from the top of the hydrogel, and washed with PBS (2 x 150 µL). The pre-prepared stain solution (100 µL) was pipetted on top of the hydrogel and incubated at 37 °C for 30 min. Then, the staining solution on top of the hydrogel was removed, and was further washed with PBS (2 x 150 µL). An additional volume of PBS (100 µL) was added on top of the hydrogel before imaging. Fluorescent Z-stack images (~80 images/per sample) through the gel were acquired on a Zeiss LSM 710 confocal laser scanning

microscope using 488 nm for excitation of calcein AM and 532 nm for excitation of the PI dye.
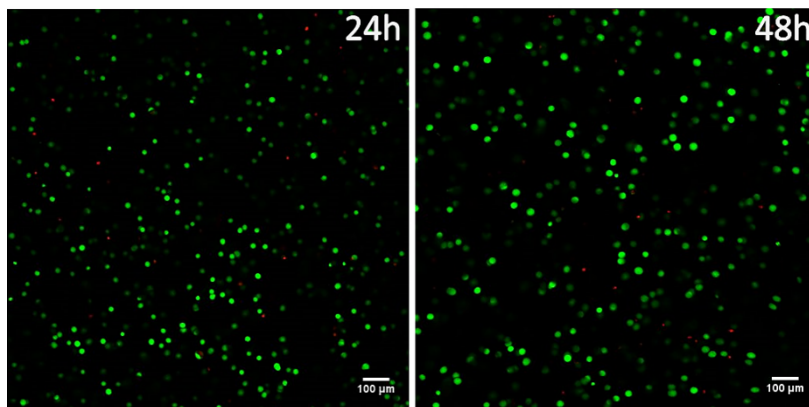

Figure S4.29 Representative confocal microscopy images of NIH 3T3 cells after 24 h and 48 h encapsulation in 3D in the DT-NB hydrogels (2.0 mM **PEGdiDT**-2.0 mM **PEGdiNB**-1.0 mM **LAP**) with 2 min UV irradiation using a benchtop LED (~10 mW/cm², 375 nm). Scale bar: *100 µm*. Green: *viable cells*, red: d*ead cells*.

4.6.9 Photo-patterning of a cell adhesive peptide

Photo-patterning using a photomask

The well inserts for seeding the hydrogels were cut from polydimethylsiloxane (PDMS) sheets produced on silicon wafers. A silicon wafer was first silanized by chemical vapour deposition of 1H,1H,2H,2Hperfluorooctyltrichlorosilane under vacuum for one hour to ensure proper PDMS detachment later. The precrosslinked PDMS was spin-coated on top of the silicon wafer to ensure a constant height of the polymer prior to its mixing at a 1:10 ratio with the crosslinker5 before baking at 100 °C for 6 hours. The custom-made wells were washed with 70% ethanol, dried, cut, and placed inside an uncoated 8-well cell culture plate. Each imaging chamber was exposed to UV-ozone surface treatment for 30 min to increase the surface hydrophilicity of the 8-well cell culture plate before use.

The hydrogel of **PEGdiDT-PEGdiNB** (3.0 mM **PEGdiDT**-3.0 mM **PEGdiNB**-1.0 mM **LAP**) (150 µL) was prepared according to the following: the precursor solution (10 µL) was pipetted into the well inserts as prepared above and irradiated with UV light for 3 min using a benchtop LED source (~10 mW/cm², 375 nm). The formed hydrogel was washed with PBS (2 x 200 µL). Then, a solution

(150 µL) containing 0.5 mM **(Fluorescein)GK(DT)GGGRGDS** and 1.0 mM **LAP** was layered on top of the hydrogel and incubated at 25 °C for 2 h to enable its diffusion into the hydrogel, followed by removing the excess solution afterwards and washing with PBS (2 x 200 µL). The hydrogel was photo-patterned using UV-irradiation for 2 min using an anti-reflective chrome photomask. Finally, the patterned hydrogels were washed with PBS (200 µL) every hour over a 6 h period incubated at 25 °C. The hydrogels were further incubated at 25 °C in PBS (200 µL) overnight before imaging.

Two-photon crosslinking using direct laser writing

Identical to the photo-patterning experiments using a mask-based approach, pre-gel precursor solutions of **PEGdiDT-PEGdiNB** (3.0 mM **PEGdiDT**-3.0 mM **PEGdiNB**-1.0 mM **LAP**) were pipetted into custom cut PDMS inserts placed on glass microscope coverslips (#1.5, 30 mm, Thermo Fisher Scientific) using 3 min UV irradiation from a benchtop LED source (~10 mW/cm^2, 375 nm) to trigger hydrogel formation. Then, a solution (50 µL) containing 0.5 mM **(Fluorescein)GK(DT)GGGRGDS** and 1.0 mM **LAP** was layered on top of the hydrogel and incubated for 2 h at 25 °C, followed by washing with PBS (2 x 100 µL). The hydrogels were kept immersed in 50-100 µL PBS. The PDMS well-inserts were sealed with a second glass coverslip to prevent evaporation during the direct laser writing process.

Two-photon crosslinking by direct laser writing (DLW) was performed using the Photonics Professional GT (Nanoscribe GmbH). 3D structures were designed in Autodesk Inventor (Autodesk) and converted to the stereolithography file format (STL). Then, STL files were imported into DeScribe (Nanoscribe GmbH) to obtain a suitable mesh for DLW. The hydrogel and crosslinker composite were exposed to a 780 nm laser (Ti-Sapphire, 20 mW maximum at sample surface) using a 20x Air objective. In the x, y-directions the DLW mesh was scanned by the laser through galvanic mirrors, and then stitched, slice-by-slice, in the z-direction with a piezo stage. The scanning speed was set at 500 µm/s with a power scaling 0.75. All DLW procedures were performed under yellow light (λ = 577-597 nm) to prevent spontaneous cross-linking during the writing process. The samples were washed 5x with PBS and kept in DPBS after two-photon crosslinking.

Confocal microscopy imaging of photo-patterned and two-photon crosslinked hydrogels

The photo-patterned and two-photon crosslinked hydrogels with cell adhesive peptides were imaged using a 10x objective on a Nikon Eclipse Ti microscope equipped with a Yokogawa confocal spinning disk unit operated at 10,000 rpm (Nikon). The attached fluorescein was excited with a 0.2 mW, 488 nm laser light from a solid-state diode laser (Coherent) supported in an Agilent MLC4 unit (Agilent Technologies). Images were captured using an exposure time of 300 ms by an Andor iXon Ultra 897 High Speed EM-CCD camera (Andor Technology). The acquired fluorescent images were background corrected to visualize the sections that underwent crosslinking.
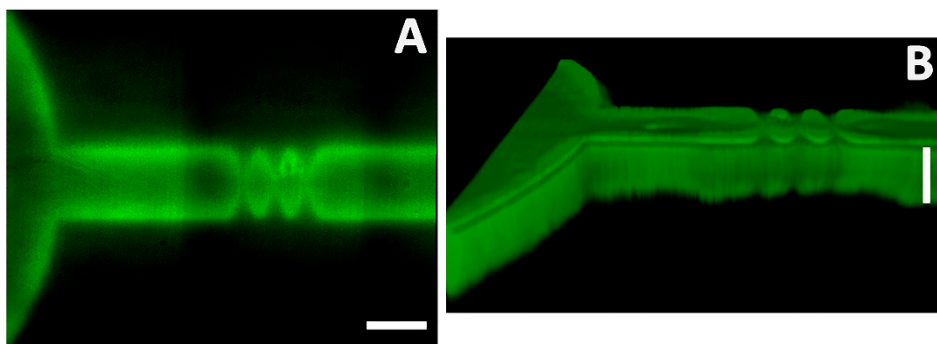
Figure S4.30 (A) 2D and (B) 3D confocal fluorescence images of fluorescein-labeled RGD peptide (**(fluorescein)GK(DT)GGGRGDS**) patterned in pre-prepared **PEGdiDT-PEGdiNB** hydrogels (3.0 mM **PEGdiDT**-3.0 mM **PEGdiNB**-1.0 mM **LAP**). Scale bar: *200 μm*.

4.6.10 References

(1) Perera, M. M.; Ayres, N. *Polym. Chem.* **2017**, *8* (44), 6741-6749.
(2) Yu, H.; Wang, Y.; Yang, H.; Peng, K.; Zhang, X. *J. Mater. Chem. B* **2017**, *5* (22), 4121-4127.
(3) Fairbanks, B. D.; Schwartz, M. P.; Halevi, A. E.; Nuttelman, C. R.; Bowman, C. N.; Anseth, K. S. *Adv.Mater.* **2009**, *21* (48), 5005-5010.
(4) Yang, F.; Wang, J.; Cao, L.; Chen, R.; Tang, L.; Liu, C. *J. Mater. Chem. B* **2014**, *2* (3), 295-304.
(5) Efimenko, K.; Wallace, W. E.; Genzer, J. *J. Colloid Interface Sci.* **2002**, *254* (2), 306-315.